

# Chapter 3

## Methods of analysis of confined many-particle systems

In the previous Chapter I have presented a detailed description of single-particle properties of nanostructures with various symmetries. It was the first, necessary step towards the main goal of this work - a description of the behaviour of *many particles* confined in these potentials, with a special emphasis put on correlation effects. To be able to achieve this goal, I have to develop methods capable of describing the systems of many interacting particles with sufficient accuracy. This Chapter contains a detailed presentation of my method of choice - the exact diagonalisation technique. I have chosen this method because, if properly used, it allows to account for all the interaction effects: direct and exchange Coulomb terms as well as particle-particle correlations, since the results it produces are *exact*.

My description will start with the mean-field Hartree-Fock approximation, accounting only for the direct and exchange Coulomb terms. Then I will begin the construction of the exact diagonalisation method by discussing two different ways of constructing the many-particle basis set: configurations of electrons distributed on single-particle states,

and configurations of quasiparticles distributed on Hartree-Fock orbitals. I shall also discuss possible optimisations of this basis set, obtained by explicitly accounting for all the symmetries of the system. I shall also compare this method with other approaches, more approximate and less controllable, but nevertheless capable of accounting for the correlations. These methods are the density functional theory in the local spin density approximation, and the quantum Monte Carlo method.

But before I move on to the methods, I will first formulate a general definition of the problem of many interacting particles confined by a QD potential.

## 3.1 The problem of many interacting particles in a QD confinement

### 3.1.1 The many-particle Hamiltonian

The Hamiltonian of  $N$  interacting electrons confined by the potential  $U(\mathbf{r})$  of the nanostructure and in the presence of an external magnetic field can be written in the form:

$$\hat{H} = \sum_{i=1}^N \left[ \frac{1}{2m^*} \left( \hat{\mathbf{p}}_i + \frac{e}{c} \mathbf{A}_i \right)^2 + U(\mathbf{r}_i) \right] + \frac{1}{2} \sum_{i \neq j}^N \frac{e^2}{\varepsilon |\mathbf{r}_i - \mathbf{r}_j|}, \quad (3.1)$$

where the notation corresponds to that introduced in Chapter 2. The first term in the above Hamiltonian introduces the single-particle QD spectrum for each confined particle, and has been considered in the previous Chapter. The second term is new - it describes the particle-particle Coulomb interactions.

The notation of my analysis will become particularly simple if I express the Hamiltonian in the language of the fermionic creation and annihilation operators. They will be denoted by  $c_{i\sigma}^+$  and  $c_{i\sigma}$ , respectively. These operators create (annihilate) a particle on the single-particle orbital  $i$  with spin  $\sigma$ . Here  $i$  is a composite orbital index, denoting  $(n, m)$  in the case of the parabolic potential,  $(n, m, l)$  in the case of the quantum disk, and  $m$  in

the case of the quantum ring. In the language of these operators the Hamiltonian takes a simpler form

$$\hat{H} = \sum_{i\sigma} E(i, \sigma) c_{i\sigma}^+ c_{i\sigma} + \frac{1}{2} \sum_{ijkl\sigma\sigma'} \langle i\sigma, j\sigma' | V | k\sigma', l\sigma \rangle c_{i\sigma}^+ c_{j\sigma'}^+ c_{k\sigma'} c_{l\sigma}. \quad (3.2)$$

Now the summation extends over all single-particle orbitals.

Creation operators also allow for a concise notation regarding many-particle states. In their language, a configuration obtained by distributing  $N$  electrons on single-particle orbitals can be written as

$$|i_1\sigma_1, i_2\sigma_2, \dots, i_N\sigma_N\rangle = c_{i_1\sigma_1}^+ c_{i_2\sigma_2}^+ \dots c_{i_N\sigma_N}^+ |0\rangle, \quad (3.3)$$

where  $|0\rangle$  denotes the vacuum. The equivalent of the above configuration, written in real space, is the Slater determinant built out of orbitals  $i\sigma$ . The antisymmetry of the state is guaranteed by the Fermionic anticommutation rules of the creation and annihilation operators:

$$\{c_i^+, c_j^+\} = \{c_i, c_j\} = 0; \quad \{c_i, c_j^+\} = \delta_{ij}. \quad (3.4)$$

The configurations constructed in such a way are not eigenstates of the many-body Hamiltonian (3.2), since these states are built out of the single-particle orbitals, and the Coulomb interaction can scatter particles between these orbitals. But the exact eigenstates of the interacting system can be written as *linear combinations* of many such configurations. The question of what these combinations should be is the central question of this thesis.

To complete my definition of the many-body problem, I have to define the Coulomb matrix element  $\langle i, j | V | k, l \rangle$  appearing in the Hamiltonian (3.2). In general these matrix elements can be constructed by carrying out the real-space integration:

$$\langle i\sigma, j\sigma' | V | k\sigma', l\sigma \rangle = \frac{e^2}{\varepsilon} \int d\mathbf{r}_1 \int d\mathbf{r}_2 \frac{\Psi_{i\sigma}^*(\mathbf{r}_1) \Psi_{j\sigma'}^*(\mathbf{r}_2) \Psi_{k\sigma'}(\mathbf{r}_2) \Psi_{l\sigma}(\mathbf{r}_1)}{|\mathbf{r}_1 - \mathbf{r}_2|}. \quad (3.5)$$

In the remainder of this thesis I will be particularly interested in the matrix elements in the parabolic confinement. The orbitals  $\Psi(\mathbf{r})$  are then the harmonic-oscillator states. In this case the matrix elements can be obtained analytically in a closed form. I shall present a detailed description of their evaluation in the next Section.

### 3.1.2 Coulomb matrix elements in the harmonic-oscillator basis

In this Section I calculate analytically the electron-electron Coulomb scattering matrix elements in the basis of the two-dimensional harmonic-oscillator orbitals. This calculation is similar to that presented in Ref. [127]. The final form of the Coulomb matrix elements in this basis was first given in Ref. [52], and later also reported in Ref. [34, 70].

In the units of effective Rydberg and effective Bohr radius (see Section 2.2) the part of the Hamiltonian (3.2) describing the electron-electron Coulomb scattering can be written as:

$$H_C = \frac{1}{2} \sum_{ijkl\sigma\sigma'} \langle i\sigma j\sigma' | v | k\sigma' l\sigma \rangle c_{i\sigma}^+ c_{j\sigma'}^+ c_{k\sigma'} c_{l\sigma}, \quad (3.6)$$

where

$$v(|\mathbf{r}_1 - \mathbf{r}_2|) = \frac{2}{|\mathbf{r}_1 - \mathbf{r}_2|}, \quad (3.7)$$

and the composite indices in the harmonic-oscillator basis  $i = (n'_1, m'_1)$ ,  $j = (n'_2, m'_2)$ ,  $k = (n_2, m_2)$ ,  $l = (n_1, m_1)$ .

Further I will use the coordinates  $x$  and  $y$  of each particle written in the language of the harmonic-oscillator lowering and raising operators introduced in Section 2.1:

$$x = \frac{\ell}{\sqrt{2}} (a + a^+ + b + b^+), \quad y = \frac{i\ell}{\sqrt{2}} (a - a^+ - b + b^+). \quad (3.8)$$

Let us start the analysis by unfolding the Coulomb interaction into the basis of plane waves. In what follows I shall suppress the spin index  $\sigma$  of the orbitals, as it will play no role in this derivation.

$$\begin{aligned} \langle ij | v | kl \rangle &= \langle i | \langle j | \sum_q v_q e^{i\mathbf{q}(\mathbf{r}_1 - \mathbf{r}_2)} | k \rangle | l \rangle \\ &= \sum_q v_q \langle i | \langle j | e^{i\mathbf{q}(\mathbf{r}_1 - \mathbf{r}_2)} | k \rangle | l \rangle = \sum_q v_q \langle i | e^{i\mathbf{q}\mathbf{r}_1} | l \rangle \langle j | e^{-i\mathbf{q}\mathbf{r}_2} | k \rangle, \end{aligned} \quad (3.9)$$

with  $v_q = \frac{4\pi}{q}$  being the Fourier transform of the Coulomb term. This transform is calculated in the following way:

$$v_q(q) = \int d\mathbf{r} \frac{2}{\mathbf{r}} e^{-i\mathbf{q}\mathbf{r}} = 2 \int_0^\infty r dr \int_0^{2\pi} d\phi_r \frac{1}{r} e^{-iqr \cos(\phi_r - \phi_q)}$$

$$\begin{aligned}
&= 2 \int_0^\infty dr \int_0^{2\pi} d\phi_r \sum_{m=-\infty}^{\infty} (-i)^m e^{-im(\phi_r - \phi_q)} J_m(rq) \\
&= 4\pi \int_0^\infty dr J_0(qr) = \frac{4\pi}{q}.
\end{aligned} \tag{3.10}$$

Let us calculate the first term of the sum (3.9). Substituting the equations (3.8) I get the form of the exponent:

$$\begin{aligned}
e^{i\mathbf{q}\mathbf{r}_1} &= e^{i\left(\frac{q_x \ell}{\sqrt{2}}(a_1 + a_1^\dagger + b_1 + b_1^\dagger) + i\frac{q_y \ell}{\sqrt{2}}(a_1 - a_1^\dagger - b_1 + b_1^\dagger)\right)} \\
&= e^{iQ^* a_1^\dagger + iQ a_1 + iQ b_1^\dagger + iQ^* b_1},
\end{aligned} \tag{3.11}$$

with  $Q = \frac{\ell}{\sqrt{2}}(q_x + iq_y)$ . To disentangle the operators I will use the Trotter-Suzuki formula:

$$e^{\hat{A} + \hat{B}} = e^{\hat{A}} e^{\hat{B}} e^{-\frac{1}{2}[\hat{A}, \hat{B}]}, \tag{3.12}$$

applicable under condition  $[\hat{A}, [\hat{A}, \hat{B}]] = [\hat{B}, [\hat{A}, \hat{B}]] = 0$ . I have  $[a_1^{(+)}, b_1^{(+)}] = 0$ , and  $[iQ^* a_1^\dagger, iQ a_1] = |Q|^2$  and also  $[iQ b_1^\dagger, iQ^* b_1] = |Q|^2$ , so the conditions for the applicability of the formula are satisfied for each pair of operators. I can now write

$$e^{iQ^* a_1^\dagger + iQ a_1 + iQ b_1^\dagger + iQ^* b_1} = e^{-|Q|^2} e^{iQ^* a_1^\dagger} e^{iQ a_1} e^{iQ b_1^\dagger} e^{iQ^* b_1}. \tag{3.13}$$

Analogously, only with the exception to sign in the exponent, I can write for the second particle (second term in the sum (3.9)):

$$e^{-i\mathbf{q}\mathbf{r}_2} = e^{-|Q|^2} e^{-iQ^* a_2^\dagger} e^{-iQ a_2} e^{-iQ b_2^\dagger} e^{-iQ^* b_2}. \tag{3.14}$$

Let us continue with the first particle. I need to calculate the element

$$\begin{aligned}
M_1 &= \langle i | e^{-|Q|^2} e^{iQ^* a_1^\dagger} e^{iQ a_1} e^{iQ b_1^\dagger} e^{iQ^* b_1} | l \rangle \\
&= \frac{1}{\sqrt{n_1! m_1'! n_1! m_1!}} \\
&\times \langle 00 | b_1^{m_1'} a_1^{n_1'} e^{-|Q|^2} e^{iQ^* a_1^\dagger} e^{iQ b_1^\dagger} \hat{\mathbf{1}} e^{iQ a_1} e^{iQ^* b_1} (a_1^\dagger)^{n_1} (b_1^\dagger)^{m_1} | 00 \rangle
\end{aligned} \tag{3.15}$$

(there has been a slight rearrangement of order of operators - I can do that, since operators  $a$  and  $b$  commute). The unit operator

$$\hat{\mathbf{1}} = \sum_{p_1=0}^{\infty} \sum_{p_2=0}^{\infty} |p_1 p_2\rangle \langle p_2 p_1| = \frac{1}{p_1! p_2!} \sum_{p_1=0}^{\infty} \sum_{p_2=0}^{\infty} (a_1^\dagger)^{p_1} (b_1^\dagger)^{p_2} |00\rangle \langle 00| (b_1)^{p_2} (a_1)^{p_1}.$$

I will also unfold the exponential operators in Taylor series, e.g:

$$e^{iQa_1} = \sum_{s=0}^{\infty} \frac{(iQ)^s}{s!} a_1^s. \quad (3.16)$$

In this notation it is now clear that the indices  $p_1$  and  $p_2$  can change only from 0 to  $\min(n_1, n'_1)$  and from 0 to  $\min(m_1, m'_1)$ , respectively. This is due to the fact that whenever these upper limits are exceeded, there will occur a situation when the lowering operator  $a$  or  $b$  will act on the lowest oscillator mode, giving zero as a result. Moreover, the matrix element will be nonzero only for certain powers of operators  $a$ ,  $a^+$ ,  $b$  and  $b^+$ :

$$\begin{aligned} M_1 &= \frac{1}{\sqrt{n'_1! m'_1! n_1! m_1!}} \sum_{p_1=0}^{\min(n_1, n'_1)} \sum_{p_2=0}^{\min(m_1, m'_1)} \frac{e^{-|Q|^2}}{p_1! p_2!} \\ &\times \langle 00 | b_1^{m'_1} a_1^{n'_1} \frac{(iQ^*)^{n'_1-p_1}}{(n'_1-p_1)!} (a_1^+)^{n'_1-p_1} \frac{(iQ)^{m'_1-p_2}}{(m'_1-p_2)!} (b_1^+)^{m'_1-p_2} (a_1^+)^{p_1} (b_1^+)^{p_2} | 00 \rangle \\ &\times \langle 00 | (b_1)^{p_2} (a_1)^{p_1} \frac{(iQ)^{n_1-p_1}}{(n_1-p_1)!} (a_1)^{n_1-p_1} \frac{(iQ^*)^{m_1-p_2}}{(m_1-p_2)!} (b_1)^{m_1-p_2} (a_1^+)^{n_1} (b_1^+)^{m_1} | 00 \rangle. \end{aligned} \quad (3.17)$$

From the above formula it can be seen why I chose these particular terms from the Taylor expansion of exponents - right now the operators are aligned exactly to take the state from  $|00\rangle$  on the right-hand side to  $|n'_1 m'_1\rangle$  (or  $|n_1 m_1\rangle$ ) and back. This is also why the application of all these operators will result simply in multiplicative term  $n'_1! m'_1! n_1! m_1!$ . This is in accordance to the rules of application of the raising and lowering operators, laid out in Eq. (2.15). As a result one obtains:

$$\begin{aligned} M_1 &= \frac{e^{-|Q|^2}}{\sqrt{n'_1! m'_1! n_1! m_1!}} \sum_{p_1=0}^{\min(n_1, n'_1)} \sum_{p_2=0}^{\min(m_1, m'_1)} p_1! p_2! \binom{n'_1}{p_1} \binom{n_1}{p_1} \binom{m'_1}{p_2} \binom{m_1}{p_2} \\ &\times (iQ^*)^{n'_1-p_1} (iQ)^{m'_1-p_2} (iQ)^{n_1-p_1} (iQ^*)^{m_1-p_2}. \end{aligned} \quad (3.18)$$

The matrix element for the second particle,  $M_2$ , can be calculated analogously, and will look similarly to  $M_1$ , only wherever I have the imaginary constant  $i$  in  $M_1$ , I will have  $(-i)$  in  $M_2$ . The formula for  $M_2$  will also contain new indices of summation,  $p_3$  and  $p_4$ .

Now I am able to put all the elements together and calculate

$$\langle ij | v | kl \rangle = \frac{1}{4\pi^2} \int_0^\infty q dq \int_0^{2\pi} d\phi_q \frac{4\pi}{q} M_1 M_2$$

$$\begin{aligned}
&= \frac{1}{\sqrt{n_1!m_1!n_1!m_1!n_2!m_2!n_2!m_2!}} \sum_{p_1=0}^{\min(n_1, n_1')} p_1! \binom{n_1'}{p_1} \binom{n_1}{p_1} \\
&\times \sum_{p_2=0}^{\min(m_1, m_1')} p_2! \binom{m_1'}{p_2} \binom{m_1}{p_2} \sum_{p_3=0}^{\min(n_2, n_2')} p_3! \binom{n_2'}{p_3} \binom{n_2}{p_3} \sum_{p_4=0}^{\min(m_2, m_2')} p_4! \binom{m_2'}{p_4} \binom{m_2}{p_4} \\
&\times \frac{1}{\pi} I_{p_1 p_2 p_3 p_4}, \tag{3.19}
\end{aligned}$$

where the integral

$$\begin{aligned}
I_{p_1 p_2 p_3 p_4} &= \int_0^\infty dq \int_0^{2\pi} d\phi_q e^{-2|Q|^2} (iQ^*)^{n_1-p_1} (iQ)^{m_1-p_2} (iQ)^{n_1-p_1} (iQ^*)^{m_1-p_2} \\
&\times (-iQ^*)^{n_2-p_3} (-iQ)^{m_2-p_4} (-iQ)^{n_2-p_3} (-iQ^*)^{m_2-p_4}. \tag{3.20}
\end{aligned}$$

To solve this integral I take the following steps:

1. Change of variables: I have  $Q = \frac{\ell}{\sqrt{2}}(q_x + iq_y)$ . Let us write  $Q$  in the exponential form:  $Q = |Q|e^{i\phi_q} = \frac{\ell}{\sqrt{2}}qe^{i\phi_q}$ . I want then to set  $|Q| = \frac{\ell}{\sqrt{2}}q$ , so  $dq = d|Q|\frac{\sqrt{2}}{\ell}$ . The angle is not affected. Further I drop the modulus sign by  $|Q|$ .

2. Collect the moduli of  $Q$  (not including the sign) - I get

$$Q^{n_1+m_1+n_1+m_1+n_2+m_2+n_2+m_2-2p_1-2p_2-2p_3-2p_4},$$

3. Collect the phases of  $Q$  - I get  $e^{i\phi_q(-n_1+m_1+n_1-m_1-n_2+m_2+n_2-m_2)}$

4. Collect the imaginary units  $i$ . I pick up all imaginary units (not including the sign)

$$\text{and I get } (i)^{n_1+m_1+n_1+m_1+n_2+m_2+n_2+m_2-2p_1-2p_2-2p_3-2p_4}.$$

5. And finally collect the factors  $(-1)$  appearing for the second particle - I get  $(-1)^{n_2+m_2+n_2+m_2-2p_3-2p_4}$

$$= (-1)^{n_2+m_2+n_2+m_2}, \text{ because the other two terms in exponent are even.}$$

My integral separates now into two integrals - the one over  $Q$  and the one over  $\phi_q$ . Let us carry out the second one first. I get

$$\int_0^{2\pi} d\phi_q e^{i\phi_q(-n_1+m_1+n_1-m_1-n_2+m_2+n_2-m_2)} = 2\pi \delta_{R_L, R_R}, \tag{3.21}$$

where  $R_L = (m'_1 + m'_2) - (n'_1 + n'_2)$  is the angular momentum of the pair of particles on the left hand side of the matrix element (particles on orbitals  $i$  and  $j$ ), and  $R_R = (m_1 + m_2) - (n_1 + n_2)$  is the angular momentum of the pair on the right side (particles on orbitals  $k$  and  $l$ ). I have formally obtained the **angular momentum conservation rule**.

From this rule I also obtain the identity  $n_1 + n_2 + m'_1 + m'_2 = n'_1 + n'_2 + m_1 + m_2$ . It means that the long sums in the exponents of  $Q$  and  $i$  can be written as  $n'_1 + n'_2 + m'_1 + m'_2 + n_1 + n_2 + m_1 + m_2 - 2p_1 - 2p_2 - 2p_3 - 2p_4 = 2(n'_1 + n'_2 + m_1 + m_2 - p_1 - p_2 - p_3 - p_4) = 2p$ . Now the integral

$$I_{p_1 p_2 p_3 p_4} = \frac{2\pi\sqrt{2}}{\ell} \int_0^\infty dQ e^{-2Q^2} (2Q)^{2p} \left(-\frac{1}{2}\right)^p (-1)^{n'_2 + m'_2 + n_2 + m_2} \quad (3.22)$$

(in passing I multiplied and divided by  $2^p$ ). Let us do another change of variables:  $x = 2Q^2$ , so that  $dx = 4QdQ$  and  $dQ = \frac{dx\sqrt{2}}{4\sqrt{x}}$ . I get

$$\begin{aligned} I_{p_1 p_2 p_3 p_4} &= \frac{\pi}{\ell} \left(-\frac{1}{2}\right)^p (-1)^{n'_2 + m'_2 + n_2 + m_2} \int_0^\infty dx e^{-x} (x)^{p+1/2-1} \\ &= \frac{\pi}{\ell} \left(-\frac{1}{2}\right)^p (-1)^{n'_2 + m'_2 + n_2 + m_2} \Gamma(p + 1/2). \end{aligned} \quad (3.23)$$

The symbol  $\Gamma$  denotes the Gamma function, which is the generalised factorial [1]. Now I can collect everything together.

$$\begin{aligned} \langle n'_1 m'_1, n'_2 m'_2 | v | n_2 m_2, n_1 m_1 \rangle &= \frac{1}{\ell} \frac{\delta_{R_L, R_R} (-1)^{n'_2 + m'_2 + n_2 + m_2}}{\sqrt{n'_1! m'_1! n_1! m_1! n'_2! m'_2! n_2! m_2!}} \\ &\times \sum_{p_1=0}^{\min(n_1, n'_1)} p_1! \binom{n'_1}{p_1} \binom{n_1}{p_1} \sum_{p_2=0}^{\min(m_1, m'_1)} p_2! \binom{m'_1}{p_2} \binom{m_1}{p_2} \\ &\times \sum_{p_3=0}^{\min(n_2, n'_2)} p_3! \binom{n'_2}{p_3} \binom{n_2}{p_3} \sum_{p_4=0}^{\min(m_2, m'_2)} p_4! \binom{m'_2}{p_4} \binom{m_2}{p_4} \\ &\times \left(-\frac{1}{2}\right)^p \Gamma\left(p + \frac{1}{2}\right). \end{aligned} \quad (3.24)$$

As can be seen, the Coulomb scattering matrix element in the harmonic-oscillator basis can be expressed as a sum of generalised factorials. Let us write out explicitly some of these elements. The most important one is the one with all indices equal to 0, i.e.,

$$\langle 00, 00 | v | 00, 00 \rangle = \frac{\sqrt{\pi}}{\ell} \equiv E_0 = \frac{\mathcal{E}_0}{\sqrt{2}}. \quad (3.25)$$



Here  $\mathcal{E}_0$  is the unit of exchange energy on the lowest Landau level, defined as

$$\mathcal{E}_0 = \sum_{m=0}^{\infty} \langle 00, 0m | v | 00, 0m \rangle = \frac{\sqrt{2\pi}}{\ell}. \quad (3.26)$$

I choose the quantity  $E_0$  as the unit of Coulomb energy, and express all other Coulomb matrix elements in its terms. For example,

$$\langle 00, 01 | v | 01, 00 \rangle = 0.75 E_0;$$

$$\langle 00, 01 | v | 00, 01 \rangle = 0.25 E_0.$$

The first of these two elements is the direct Coulomb term describing the repulsion of two electrons, one occupying the orbital  $(n, m) = (0, 0)$ , and the other - the orbital  $(n, m) = (0, 1)$ . This repulsion term is always nonzero, even if these electrons have opposite spins. However, the second element describes the Coulomb *exchange* between the two electrons, and it is nonzero only if the electrons have parallel spins. These spin selection rules directly follow from the form of the matrix element shown e.g. in Eq. (3.5). The spin of the two “inner” orbitals (the ones described by  $j$  and  $k$ ) must be the same, since these orbitals are integrated with respect to the same variable  $\mathbf{r}_2$ . Difference in spins would lead to orthogonality of these orbitals, and would cause the matrix element to be zero. The same is true for the two “outer” orbitals (the ones described by  $i$  and  $l$ ). These spin selection rules introduce another important symmetry of the Coulomb matrix elements. Not only do they conserve the total angular momentum of the two scattered particles, but also they conserve the  $z$  component of their total spin.

Here I shall also point out that the elements depend on the magnetic field only through the length  $\ell$  in the constant  $E_0$ . This is clearly a multiplicative constant, and Coulomb matrix elements in different magnetic fields and in potentials with different characteristic frequency  $\omega_0$  can be obtained by a simple rescaling. The fact that they do not have to be recalculated for each magnetic field and each potential makes these matrix elements very useful in large-scale calculations, as I shall demonstrate later in this work.

The last remark concerns the numerical stability of the elements  $\langle i, j | v | k, l \rangle$ . As can be seen from Eq. (3.24), these elements are long sums of factorials with alternating signs.

For higher harmonic-oscillator orbitals most of these factorial terms become very large in magnitude, but they have to reduce to a final value of order of 1 (and in practice even smaller, since the element  $\langle 00, 00|v|00, 00\rangle$  has the largest value of all the Coulomb elements). Since the present-day computers can only store a finite amount of significant digits per number, the matrix elements involving higher and higher orbitals will carry greater and greater error. Interestingly, the accumulation of this error tends to *lower* the total energy of the system. To avoid this spurious result, the matrix elements must be calculated using computers with higher precision capabilities (for instance, quadruple precision) or software packages capable of processing numbers with arbitrary precision (such as *Mathematica* or *Maple*). In my calculations I have used the C++ high-precision package called NTL, written by Victor Shoup [113].

## 3.2 The Hartree-Fock method

In Chapter 2 I have discussed the single-particle spectra of typical QD potentials, and in the previous Section I have shown how the Coulomb scattering matrix elements can be calculated for one of them - the parabolic lateral confinement. At this point all terms of the Hamiltonian (3.2), describing the system of many interacting particles confined in a QD, are known, and I may start analysing the properties of this system. However, as I have already mentioned, the many-body problem defined by the Hamiltonian (3.2) is very difficult to solve, and special methods have to be developed in order to account for all aspects of the Coulomb interactions. The rest of this Chapter will be devoted to describing these methods in detail.

I start the presentation of methods with the mean-field Hartree-Fock approximation. This effective mean-field approach accounts for the direct and exchange Coulomb interactions, but does not capture the correlation effects. In spite of that this method is of interest, for two main reasons. First, its results can be compared to those obtained using

more sophisticated approaches, which allows to isolate the effects introduced by correlations from those due to the direct and exchange terms. The second reason has to do with the form in which I write the exact eigenstates of my interacting system. In the beginning of this Chapter I have mentioned that the exact eigenstates of the Hamiltonian (3.2) can be written as linear combinations of configurations  $c_{i_1\sigma_1}^+ c_{i_2\sigma_2}^+ \dots c_{i_N\sigma_N}^+ |0\rangle$ , created using the single-particle orbitals. In the regime of strong interactions I deal with strong configuration mixing, which causes these linear combinations to involve many terms. However, instead of distributing the particles on single-particle orbitals, I can also build my configurations by distributing the quasiparticles dressed in interactions on the effective Hartree-Fock orbitals. Since these orbitals already partially account for Coulomb interactions, the configuration mixing in this case is weaker, and one may expect that good approximations of the eigenstates of the system will take the form of linear combinations with fewer terms.

The Hartree-Fock approximation is usually formulated in real space, and involves self-consistent solving for the renormalised orbitals of each electron in the presence of the external confinement and the effective potential created by the Coulomb direct and exchange interactions with all other electrons [19]. In my approach I use the language of creation operators, and write the wave function of the  $N$ -electron system as a single Slater determinant in the following form:

$$|\Psi\rangle = A_{i_1}^+ A_{i_2}^+ \dots A_{i_N}^+ |0\rangle. \quad (3.27)$$

The operators  $A_i^+$  create a particle on the Hartree-Fock orbital  $i$ , and can be written in terms of the single-particle creation operators as

$$A_i^+ = \sum_{j\sigma} a_{j\sigma}^{*(i)} c_{j\sigma}^+. \quad (3.28)$$

The complex coefficients  $a_{j\sigma}^{(i)}$  are variational parameters of the procedure. They are chosen so as to minimise the expectation value  $\langle\Psi|H|\Psi\rangle$  of the Hamiltonian 3.2 under two

constraints: (i) that the state  $|\Psi\rangle$  be normalised, and (ii) that the operators  $A_i, A_i^+$  satisfy the Fermionic anticommutation rules.

In general, the Hartree-Fock operators defined in Eq. (3.28) can involve the single-particle creation operators of all orbitals  $j$  and both spin orientations. This approach is called the spin- and space-unrestricted Hartree-Fock method [17, 133, 134]. However, since the Hamiltonian (3.2) conserves both total angular momentum and projection of the total spin, in my calculations I use the spin- and space-restricted Hartree-Fock approach, in which the creation operators  $A^+$  are written using the single-particle creation operators  $c^+$  with the same angular momentum and spin. For the parabolic potential the single-particle angular momentum  $l = n - m$ , and, for  $l \leq 0$ ,

$$A_{il\sigma}^+ = a_{0,-l,\sigma}^{*(i)} c_{0,-l,\sigma}^+ + a_{1,(-l+1),\sigma}^{*(i)} c_{1,(-l+1),\sigma}^+ + a_{2,(-l+2),\sigma}^{*(i)} c_{2,(-l+2),\sigma}^+ + \dots \quad (3.29)$$

For positive angular momenta the Hartree-Fock creation operators take a similar form:

$$A_{il\sigma}^+ = a_{l,0,\sigma}^{*(i)} c_{l,0,\sigma}^+ + a_{(l+1),1,\sigma}^{*(i)} c_{(l+1),1,\sigma}^+ + a_{(l+2),2,\sigma}^{*(i)} c_{(l+2),2,\sigma}^+ + \dots \quad (3.30)$$

Thus, the Hartree-Fock orbitals can renormalise only within a defined angular momentum and spin channel.

The coefficients  $a_{nm\sigma}^*$  are determined by minimising the expectation value  $\langle \Psi | H | \Psi \rangle$  of the many-body Hamiltonian. In the case of the spin- and space-restricted Hartree-Fock approach formulated in the language of creation operators, the minimisation procedure can be reduced to an eigenvalue problem of the Hartree-Fock Hamiltonian for each angular momentum-spin channel separately. I shall describe this procedure in detail in Chapter 5, where I use the Hartree-Fock approximation to analyse the properties of a  $N$ -electron parabolic quantum dot in an external magnetic field.

### 3.3 The exact diagonalisation approach

In the previous Section I have presented the Hartree-Fock method, capturing the direct and exchange Coulomb effects in its treatment of many confined interacting particles. I shall now move on to presenting a method that accounts for all aspects of Coulomb interactions, including electronic correlations, in an *exact* manner with controlled accuracy. This is the exact diagonalisation approach, formulated in the configuration-interaction framework.

In the configuration interaction (CI) method the Hamiltonian (3.2) is written in the matrix form in the basis of many-electron configurations. Unlike the correlated bases of Jastrow or Hylleraas functions, the configurations making up the basis do not include correlations among pairs of interacting particles, and so their repulsive interaction is not minimised. As a result, the choice and size of the CI basis affects the accuracy of the results, and, to obtain well-converged eigenenergies and eigenstates, it is usually necessary to consider very large basis sets.

In this Section I shall focus on the CI method applied to the system of  $N$  electrons confined in a parabolic quantum dot. My description starts with the choice of the many-particle basis. I shall consider two such bases, one built by distributing electrons on single-particle orbitals, and the second obtained by distributing quasiparticles on the Hartree-Fock orbitals. Then I shall move on to writing the Hamiltonian matrix in the chosen basis. I will show how the geometrical and dynamical symmetries of the single particle states, as well as the many-particle symmetries of the Hamiltonian can be exploited in order to divide the basis set into smaller, uncoupled subsets. This will allow for a reduced basis size and improved accuracy, which in turn allows for more reliable computations of many-body properties of my system in the regime of strong correlations. But, even using these reduced and optimised basis sets, the size of Hamiltonians that I need to consider is still very large (even of order of  $10^6 \times 10^6$ ). Such matrices cannot be directly stored in the memory of the present-day computers, and special methods have to be developed

to diagonalise them. One such method - the conjugate gradient approach coupled with spectrum folding - will be presented in detail.

### 3.3.1 Notation and choice of basis

#### Configurations built out of single-particle orbitals

For clarity of the discussion let us start with rewriting the Hamiltonian of the system of  $N$  interacting electrons:

$$\hat{H} = \sum_{i\sigma} E(i, \sigma) c_{i\sigma}^+ c_{i\sigma} + \frac{1}{2} \sum_{ijkl\sigma\sigma'} \langle i\sigma, j\sigma' | V | k\sigma', l\sigma \rangle c_{i\sigma}^+ c_{j\sigma'}^+ c_{k\sigma'} c_{l\sigma}. \quad (3.31)$$

Because I shall now concentrate on the case of parabolic lateral confinement, the composite index  $i$  denotes the single-particle Fock-Darwin orbital quantum numbers  $(n, m)$ .

I construct the basis of my many-particle Hilbert space out of electronic configurations by distributing my  $N$  electrons on the single-particle Fock-Darwin states in all possible ways, however obeying the Pauli exclusion principle. In the language of creation operators compatible with the Hamiltonian (3.31), such configurations will take the form:

$$|n_1 m_1 \sigma_1, n_2 m_2 \sigma_2, \dots, n_N m_N \sigma_N\rangle = c_{n_1 m_1 \sigma_1}^+ c_{n_2 m_2 \sigma_2}^+ \dots c_{n_N m_N \sigma_N}^+ |0\rangle. \quad (3.32)$$

Such configurations are orthonormal, because the single-particle Fock-Darwin orbitals are orthonormal. The only question concerns the size of this basis.

As I have shown in Section 2.1, the single-particle Fock-Darwin spectrum consists of an infinite number of levels. To be able to perform computations, I thus need to restrict the basis size, similarly as I did in Section 2.2.2: Out of the infinite number of the Fock-Darwin states I only choose a finite number  $M$  of those with the lowest energies. In the simple case of the single electron confined in a disk in a magnetic field I only needed a small number of such states (in my model 20), but I clearly stated that such a fast convergence was due to the strong zero-field quantisation brought about by the small size of the disk. Here I deal with the parabolic potential, much softer compared to that

of the disk, and I need to compare the quantisation of the single-particle energy to the characteristic energies of the Coulomb interactions. As I shall show in the next Chapter, these two energy scales are comparable, which makes it necessary to consider more single-particle levels in order to obtain a well-converged result. I shall treat the number  $M$  as a parameter controlling my approximation - the *only* approximation in the method.

Let us now find the size of the many-particle basis. I have  $N$  electrons, of which  $N_{\uparrow}$  with spin up and  $N_{\downarrow}$  with spin down, and I have to distribute them on  $M$  single-particle orbitals. Since all  $M$  single-particle states are degenerate with respect to the electron spin, the full basis size is obtained as a product

$$\text{basis size} = \binom{M}{N_{\uparrow}} \binom{M}{N_{\downarrow}}, \quad (3.33)$$

in which I simply consider distributing the spin up electrons and the spin down electrons on  $M$  levels independently (one electron of each species can occupy the same Fock-Darwin orbital).

### Configurations built out of the Hartree-Fock orbitals

The configurations constructed in the previous paragraph are Slater determinants built out of single-particle orbitals, and thus they do not include correlations between pairs of particles. Thus the particle-particle Coulomb repulsion is not minimised, which results in large diagonal and offdiagonal Hamiltonian matrix elements. This in turn entails the necessity of using very large basis sets in order to obtain accurate results.

Here I shall describe a different method of constructing the many-particle basis set: instead of distributing the electrons on the single-particle orbitals, I shall distribute the quasielectrons on the Hartree-Fock orbitals.

In Section 3.2, I have described the Hartree-Fock approximation in the language of effective creation and annihilation operators. In the space- and spin-restricted version of

the method these operators are written as

$$A_{1l\sigma}^+ = a_{n,m,\sigma}^{*(1)} c_{n,m,\sigma}^+ + a_{n+1,m+1,\sigma}^{*(1)} c_{n+1,m+1,\sigma}^+ + a_{n+2,m+2,\sigma}^{*(1)} c_{n+2,m+2,\sigma}^+ + \dots \quad (3.34)$$

$$A_{2l\sigma}^+ = a_{n,m,\sigma}^{*(2)} c_{n,m,\sigma}^+ + a_{n+1,m+1,\sigma}^{*(2)} c_{n+1,m+1,\sigma}^+ + a_{n+2,m+2,\sigma}^{*(2)} c_{n+2,m+2,\sigma}^+ + \dots \quad (3.35)$$

$$A_{3l\sigma}^+ = a_{n,m,\sigma}^{*(3)} c_{n,m,\sigma}^+ + a_{n+1,m+1,\sigma}^{*(3)} c_{n+1,m+1,\sigma}^+ + a_{n+2,m+2,\sigma}^{*(3)} c_{n+2,m+2,\sigma}^+ + \dots \quad (3.36)$$

with the angular momentum  $l = n - m$ , and coefficients  $a$  established in the Hartree-Fock minimisation. For each angular momentum and spin channel there is one-to-one correspondence between the effective creation operators  $A^+$  (and the effective annihilation operators  $A$ ) and the Fock-Darwin creation and annihilation operators  $c^+$  and  $c$ , respectively. The transformation between one set of operators and the other can be seen simply as a rotation, and let us denote the rotation matrix as  $U_{l\sigma}$ :  $A_{il\sigma}^+ = \sum_j U_{l\sigma}(i, j) c_{j\sigma}^+$ . This matrix may, in general, be different for each angular momentum and spin channel. Moreover, the operators  $A^+$  and  $A$  can be constructed not only for occupied, but also for unoccupied orbitals. This operation is outside of the Hartree-Fock procedure itself; the corresponding sets of coefficients  $a$  are the eigenvectors obtained in the diagonalisation of the Hartree-Fock matrices for all angular momentum and spin channels (including those that do not contain electrons).

By performing the rotation  $U_{l\sigma}$  I create a new, effective single-quasiparticle basis set, whose orbitals account for the direct and exchange interactions in the system. It is therefore advantageous to build my many-particle configurations in the new basis.

The construction of the many-particle basis set proceeds as follows. First I perform the Hartree-Fock procedure to find the Hartree-Fock ground state  $|\Psi\rangle$ , thereby establishing the rotation matrices  $U_{l\sigma}$ . Then I write my many-body Hamiltonian in the language of the effective creation and annihilation operators:

$$\begin{aligned} \hat{H} &= \sum_{k,k',l,\sigma} t_{kl\sigma,k'l\sigma} A_{kl\sigma}^+ A_{k'l\sigma} \quad (3.37) \\ &+ \frac{1}{2} \sum_{k_1 k_2 k_3 k_4} \sum_{l_1 l_2 l_3 l_4} \sum_{\sigma \sigma'} \langle k_1 l_1 \sigma, k_2 l_2 \sigma' | V | k_3 l_3 \sigma', k_4 l_4 \sigma \rangle A_{k_1 l_1 \sigma}^+ A_{k_2 l_2 \sigma'}^+ A_{k_3 l_3 \sigma'} A_{k_4 l_4 \sigma}. \end{aligned}$$



Note that in the basis of the effective Hartree-Fock orbitals the energy term  $t$  is not diagonal, but couples different orbitals within the same angular momentum and spin channel. The Coulomb matrix elements in the new basis are obtained by a rotation:

$$\begin{aligned} \langle k_1 l_1, k_2 l_2 | V | k_3 l_3, k_4 l_4 \rangle &= \sum_{n_1 m_1} \sum_{n_2 m_2} \sum_{n_3 m_3} \sum_{n_4 m_4} \langle n_1 m_1, n_2 m_2 | V | n_3 m_3, n_4 m_4 \rangle \\ &\times U_{l_1}(k_1, (n_1 m_1)) U_{l_2}(k_2, (n_2 m_2)) U_{l_3}^+(k_3, (n_3 m_3)) U_{l_4}^+(k_4, (n_4 m_4)). \end{aligned} \quad (3.38)$$

The summation over the Fock-Darwin indices  $(nm)$  is done under constraints  $n_1 - m_1 = l_1$ ,  $n_2 - m_2 = l_2$ ,  $n_3 - m_3 = l_3$  and  $n_4 - m_4 = l_4$ . At this point both the effective single-particle basis and the rotated Hamiltonian are known. I can proceed to distributing my quasiparticles on the Hartree-Fock orbitals and creating the configurations of the type

$$|k_1 l_1 \sigma_1, k_2 l_2 \sigma_2, \dots, k_N l_N \sigma_N \rangle = A_{k_1 l_1 \sigma_1}^+ A_{k_2 l_2 \sigma_2}^+ \dots A_{k_N l_N \sigma_N}^+ |0 \rangle. \quad (3.39)$$

From this moment on, creation of the many-particle basis and diagonalisation of the Hamiltonian is carried out exactly in the same way as it is done for the case of non-renormalised single-particle orbitals.

An alternative way of constructing the manyparticle basis set is to start with the Hartree-Fock ground state  $|\Psi\rangle$  and construct the basis vectors as quasielectron-quasihole pair excitations from this state. For example, the single-pair excitations are created as configurations of the type

$$A_{k_1 l_1 \sigma}^+ A_{k_2 l_2 \sigma'} |\Psi\rangle,$$

and can be constructed either with  $(\sigma \neq \sigma')$  or without  $(\sigma = \sigma')$  flipping the spin of the quasiparticle. Such excitations are thus obtained from the Hartree-Fock ground state by taking one quasiparticle (electron dressed in interactions) from below the Fermi energy, which creates a hole in the interior of the electronic droplet. The quasielectron is then put on one of the unoccupied Hartree-Fock orbitals above the Fermi energy. In this way I can create two- and multiple-pair excitations. Note that this approach allows to isolate the lower-lying excitations (two- and three-pair) from higher-lying ones (multiple-pair). In the exact-diagonalisation procedure the largest corrections to the energy of the

system are introduced by those basis states that are closest in energy to the ground state, as I have demonstrated in Section 2.2.2 on the example of the single-particle spectrum. Therefore it is advantageous to build my basis set from the vectors describing the few-pair excitations, as being more relevant for the accuracy of the result, and neglect the higher-pair excitations. I shall demonstrate the details of this procedure in Chapter 5, where I shall use the Hartree-Fock and exact diagonalisation methods to analyse the properties of the system of interacting electrons confined in a parabolic QD in an external magnetic field.

### 3.3.2 Exact diagonalisation method optimised for parabolic lateral confinements

From the formula (3.33) it is clear that this size grows factorially both with the number of single-particle states  $M$  and the number of electrons  $N$ . For instance, if I take six electrons, with  $N_{\uparrow} = 3$  and  $N_{\downarrow} = 3$ , and distribute them in all possible ways on  $M = 20$  orbitals, the total basis size is 1299600. This means that without further refinement I am unable to obtain any meaningful results with this method.

The optimisation of the basis set involves exploiting the symmetries of the system. I have demonstrated this idea at work already in Section 2.2.2, where I isolated subsets of the basis with definite angular momentum and definite vertical quantum number, and demonstrated that the Hamiltonian does not couple them. Because of that I could resolve the angular momentum-subband channels, and I performed the diagonalisation study in each such channel.

In the case of the many-particle system in the parabolic confinement I also have several symmetries, leading to a block-diagonal form of the Hamiltonian in the full configuration basis. The total Hamiltonian (3.31) in the basis of configurations built out of harmonic-oscillator single-particle basis conserves the total angular momentum  $L$ , total spin  $\mathbf{S}$ , and

total spin projection  $S_z$  of the system, and therefore I may classify the many-particle configurations into groups labelled by these three quantum numbers. The same is true for the Hamiltonian (3.38) in the basis of configurations built out of the effective Hartree-Fock orbitals calculated in the spin- and space-restricted approach. However, out of these two Hamiltonians only the first one exhibits an additional symmetry, stemming from the parabolic form of the confinement: it couples only the states with the same type of the centre-of-mass motion. This additional, fourth good quantum number allows to optimise the harmonic-oscillator many-particle basis set better than the one based on Hartree-Fock orbitals, and therefore in the rest of this Section I will focus on the former.

A detailed discussion of the optimisation steps applied to the many-particle basis set on the specific example of an  $N$ -electron parabolic quantum dot in a magnetic field is presented in the article “Configuration interaction method for Fock-Darwin states”, written by Andreas Wensauer, Marek Korkusiński, and Pawel Hawrylak, and published in *Solid State Communications*, vol. 130, page 115 (2004). This publication is an integral part of this thesis and is appended to the presented material. Here I will highlight its most important points.

### Angular momentum

Let us start with the conservation of total angular momentum. The total angular momentum operator is defined as

$$\hat{L} = \sum_{nm\sigma} (n - m) c_{nm\sigma}^+ c_{nm\sigma}. \quad (3.40)$$

Since the parabolic confinement is circularly symmetric, each single-particle orbital has a definite angular momentum, and therefore the operator  $\hat{L}$  commutes with the single-particle energy term (consisting of the kinetic energy operator and the external confinement potential) of the Hamiltonian (3.31). Moreover, as I have demonstrated in Section 3.1.2, the Coulomb interactions conserve the total angular momentum of the scattered

pair of particles. Thus the operator  $\hat{L}$  commutes also with the interaction term in this Hamiltonian. This allows me to group my basis configurations into subspaces according to the total angular momentum.

### Projection of the total spin

The second symmetry is the projection of the total spin  $S_z$ , whose corresponding operator is defined as:

$$\hat{S}_z = \sum_{nm\sigma} \sigma c_{nm\sigma}^+ c_{nm\sigma}. \quad (3.41)$$

In the Hamiltonian (3.31) there is only one term that couples to the spin of each electron: the single-particle Zeeman term in the single-particle energy operator. The Zeeman term, however, does not lead to spin flips, but lowers or increases the energy of a single-particle orbital depending on the magnetic field and the direction of the electronic spin. This means that the operator  $\hat{S}_z$  commutes with the total Hamiltonian, and all the configurations from each angular momentum subspace can be further grouped according to the value of their total spin projection  $S_z$ .

### Total spin

Accounting for the conservation of the total spin  $\mathbf{S}$  of the system is more complicated. The total spin is a vector quantity, and to simplify my description I will focus on its square: the operator  $\hat{S}^2$ . This operator, written in the language of creation and annihilation operators for  $N$  confined electrons, takes the form

$$\hat{S}^2 = \frac{N}{2} + \hat{S}_z^2 - \sum_{ij} c_{j\uparrow}^+ c_{i\downarrow}^+ c_{j\downarrow} c_{i\uparrow}. \quad (3.42)$$

The two first terms of the operator  $\hat{S}^2$  are diagonal, and give the same values for all the  $N$ -electron configurations from the same angular-momentum and  $S_z$ -resolved basis set. The third term, however, couples many-particle configurations in such a way that it annihilates the particle on the orbital  $i$  and recreates it on the same orbital with the flipped spin;

the same is true for particle  $j$ . Note that for the two configurations to be coupled by  $\hat{S}^2$ , they have to exhibit the same pattern of orbital quantum numbers, and only differ in the way the spin-up and spin-down electrons are distributed on these orbitals. For example, the operator  $\hat{S}^2$  couples the configuration  $|a\rangle = c_{00\uparrow}^+ c_{11\downarrow}^+ |0\rangle$  to  $|b\rangle = c_{11\uparrow}^+ c_{00\downarrow}^+ |0\rangle$ , but none of these configurations is coupled to  $|c\rangle = c_{00\uparrow}^+ c_{33\downarrow}^+ |0\rangle$ . Therefore it is possible to arrange the many-particle configurations into blocks with the same orbital pattern. I can then construct the matrix  $\hat{S}^2$  in the basis of each of these blocks and diagonalise it numerically to obtain the eigenstates of the total spin operator. For example, in the basis of my two configurations  $\{|a\rangle, |b\rangle\}$  the matrix of the operator  $\hat{S}^2$  takes the form

$$\hat{S}^2 = \begin{bmatrix} 1 & -1 \\ -1 & 1 \end{bmatrix}, \quad (3.43)$$

and, upon the diagonalisation of this simple matrix one obtains the eigenstate  $|S\rangle = \frac{1}{\sqrt{2}}(|a\rangle + |b\rangle)$  with the eigenvalue  $S^2 = 0$ , and the eigenstate  $|T\rangle = \frac{1}{\sqrt{2}}(|a\rangle - |b\rangle)$  with the eigenvalue  $S^2 = 2$ . The first eigenstate is the spin singlet, and the second - the spin triplet. To enumerate these states, usually the eigenvalue of the total spin is used instead of the eigenvalue of  $\hat{S}^2$ ; these two eigenvalues are connected via the relationship

$$\langle \hat{S}^2 \rangle = S(S + 1). \quad (3.44)$$

This means that the eigenvalue corresponding to the state  $|S\rangle$  is  $S = 0$ , and the one corresponding to the state  $|T\rangle$  is  $S = 1$ . The rotation to the basis of total spin eigenvectors becomes increasingly more complicated as the number of particles increases. The spin blocks are, however, fairly small, and are composed, e.g., of up to several hundred configurations for the system with  $N = 6$  electrons. From this simple analysis it is clear that the many-particle basis with resolved total angular momentum, total spin, and total projection of the total spin will no longer consist of many-particle configurations, but will be composed of their linear combinations.

To illustrate how resolving the total spin as a good quantum number decreases the size of the many-particle basis, let us consider the system of  $N = 6$  electrons, out of

which  $N_{\uparrow} = 3$  are spin up and  $N_{\downarrow} = 3$ , distributed on the  $M = 121$  single-particle orbitals  $(n, m)$ , for which  $0 \leq n \leq 10$  and  $0 \leq m \leq 10$ . According to the formula (3.33), by distributing these electrons on these single-particle orbitals more than  $8.29 \times 10^{10}$  many-particle configurations can be generated. Out of those configurations there are 326120 configurations with total angular momentum  $L = 0$ . Further, if I resolve the total spin as a good quantum number, I obtain 92410 configurations with  $S = 0$ , 152460 configurations with  $S = 1$ , 70711 configurations with  $S = 2$ , and 10593 configurations with  $S = 3$ . Therefore, by resolving the two quantum numbers  $L$  and  $S$  I have reduced the size of the problem of six electrons with total spin projection  $S_z = 0$  by five orders of magnitude.

### Centre of mass

Let us now move on to describing the last symmetry, involving the centre-of-mass (CM) motion of the system. The parabolic confinement allows for a separation of the CM and relative motion of  $N$  interacting confined electrons, and so the real-space Hamiltonian of the system can be written as [51, 62]:

$$\hat{H} = \hat{H}_{CM}(\mathbf{R}, \mathbf{P}) + \hat{H}_{rel}(\varrho_1, \dots, \varrho_{N-1}, \pi_1, \dots, \pi_{N-1}). \quad (3.45)$$

Here,  $N\mathbf{R} = \sum_{i=1}^N \mathbf{r}_i$  and  $\mathbf{P} = \sum_{i=1}^N \mathbf{p}_i$  are the CM coordinate and momentum, respectively, and  $\varrho_i, \pi_i$  are, respectively, the position and momentum of the  $i$ -th relative particle, which can be written using Jacobi coordinates [62]. In the following I shall focus on the CM Hamiltonian, which, when written in the real-space representation, takes the form:

$$\hat{H}_{CM} = \frac{1}{2Nm^*} \mathbf{P}^2 + \frac{1}{2} Nm^* \omega_h \mathbf{R}^2 + \frac{1}{\omega_c} 2[\mathbf{R} \times \mathbf{P}]_z. \quad (3.46)$$

The notation used in this formula follows that introduced in the Section 2.1. I can now express the CM position and momentum by the single-particle raising and lowering operators  $a^+, b^+, a$ , and  $b$ , and write the CM Hamiltonian in the second quantisation as:

$$\hat{H}_{CM} = \hbar\omega_+ \left( \hat{A}_+^\dagger \hat{A}_+ + \frac{1}{2} \right) + \hbar\omega_- \left( \hat{A}_-^\dagger \hat{A}_- + \frac{1}{2} \right), \quad (3.47)$$

where the operators  $A_{\pm}^{\dagger}$ ,  $A_{+}$ ,  $A_{-}^{\dagger}$ , and  $A_{-}$  are bosonic operators describing collective CM excitations of the system:

$$\hat{A}_{+}^{\dagger} = \frac{1}{\sqrt{N}} \sum_{nm\sigma} \sqrt{n+1} c_{(n+1)m\sigma}^{\dagger} c_{nm\sigma}; \quad (3.48)$$

$$\hat{A}_{-}^{\dagger} = \frac{1}{\sqrt{N}} \sum_{nm\sigma} \sqrt{m+1} c_{n(m+1)\sigma}^{\dagger} c_{nm\sigma}; \quad (3.49)$$

$$\hat{A}_{+} = \frac{1}{\sqrt{N}} \sum_{nm\sigma} \sqrt{n} c_{(n-1)m\sigma}^{\dagger} c_{nm\sigma}; \quad (3.50)$$

$$\hat{A}_{-} = \frac{1}{\sqrt{N}} \sum_{nm\sigma} \sqrt{m} c_{n(m-1)\sigma}^{\dagger} c_{nm\sigma}. \quad (3.51)$$

These operators can be interpreted respectively as creation and annihilation operators for collective excitations of the system. The operator  $A_{\pm}^{\dagger}$  ( $A_{\pm}$ ) increases (decreases) the total energy of the system by  $\hbar\omega_{\pm}$ , while the operator  $A_{\pm}^{\dagger}$  ( $A_{\pm}$ ) increases (decreases) the total energy of the system by  $\hbar\omega_{\pm}$ . Note that these operators do not couple to the interaction term in the many-particle Hamiltonian. The CM operators can be now constructed using the four operators defined above as:

$$\hat{C}_{+} = A_{+}^{\dagger} A_{+} = \frac{1}{N} \sum_{n'm'\sigma'nm\sigma} \sqrt{n(n'+1)} c_{(n'+1)m'\sigma'}^{\dagger} c_{n'm'\sigma'} c_{(n-1)m\sigma}^{\dagger} c_{nm\sigma}, \quad (3.52)$$

$$\hat{C}_{-} = A_{-}^{\dagger} A_{-} = \frac{1}{N} \sum_{n'm'\sigma'nm\sigma} \sqrt{m(m'+1)} c_{n'(m'+1)\sigma'}^{\dagger} c_{n'm'\sigma'} c_{n(m-1)\sigma}^{\dagger} c_{nm\sigma}. \quad (3.53)$$

These two operators commute with the total Hamiltonian.

Let us focus, for example, on the operator  $\hat{C}_{-}$ . Note that this operator affects only the pattern of orbital quantum numbers  $m$ , leaving the number  $n$  of each electron unchanged. Therefore, similarly to the case of the total spin, I can arrange the configurations into blocks. The configurations belonging to each block have the same pattern of quantum numbers  $n\sigma$ , but differ in the patterns of the numbers  $m$ . To resolve the CM quantum numbers I build the matrix corresponding to the operator  $\hat{C}_{-}$  in each block and diagonalise it numerically. As a result I obtain the eigenvectors of the total centre-of-mass operator, together with the corresponding CM quantum numbers. For further processing it is sufficient to collect only those CM eigenstates with CM eigenvalues equal to zero; all other eigenstates can be generated simply by application of the CM raising operator  $A_{\pm}^{\dagger}$ .

In the paper we apply the basis reduction rules discussed in this Section to a model case of  $N = 4 - 7$  interacting electrons confined by a parabolic potential in the absence of the magnetic field, and  $N = 4$  electrons in the magnetic field. We show that the obtained results compare well with those obtained using the quantum Monte Carlo and stochastic-variational methods. We also point out that use of the optimised configuration-interaction approach allows to calculate reliably not only the ground state, but also the excited states of the system, an ability which the two other methods lack.

### 3.3.3 Creation of the Hamiltonian matrix

I have demonstrated how I create the basis of configurations and how I can optimise it to account for the symmetries of the system. Let us now move on to describing how the Hamiltonian is written in the matrix form in this basis.

I will describe the creation of the Hamiltonian matrix on a simple example of the system of  $N = 3$  electrons, two with spin down and one with spin up. I shall restrict the number of the single-particle Fock-Darwin states available for my electrons to three:  $(n, m) = (0, 0)$ ,  $(n, m) = (0, 1)$ , and  $(n, m) = (1, 0)$ . According to Eq. (3.33), in this case I can generate nine electronic configurations with different angular momenta. To optimise this basis I focus on the states with total angular momentum  $L = -1$  only. This reduces my set to two configurations:

$$|a\rangle = c_{0,0,\downarrow}^+ c_{0,1,\downarrow}^+ c_{0,0,\uparrow}^+ |0\rangle; \quad (3.54)$$

$$|b\rangle = c_{0,1,\downarrow}^+ c_{1,0,\downarrow}^+ c_{0,1,\uparrow}^+ |0\rangle. \quad (3.55)$$

Note that in writing these two configurations I am using a convention, to which I shall adhere throughout this work: from left to right I write the creation operators first for spin-down, and then for spin-up electrons, and for each spin species I arrange the orbitals according to their energy in ascending order.

The configuration  $|a\rangle$  is composed of two electrons with antiparallel spins occupying



the orbital  $(0, 0)$  and one spin-down electron on the orbital  $(0, 1)$ . The configuration  $|b\rangle$ , on the other hand, consists of two electrons with antiparallel spins on the orbital  $(0, 1)$  and one spin-down electron on the orbital  $(1, 0)$ . Both configurations have total spin  $S = 1/2$ , so my basis set  $\{|a\rangle, |b\rangle\}$  is already composed of total spin eigenstates.

In my simple basis the Hamiltonian can be written as a  $2 \times 2$  matrix in the following form:

$$\hat{H} = \begin{bmatrix} \langle a|H|a\rangle & \langle a|H|b\rangle \\ \langle b|H|a\rangle & \langle b|H|b\rangle \end{bmatrix}. \quad (3.56)$$

My task is to calculate the matrix elements  $\langle a|H|a\rangle$ ,  $\langle a|H|b\rangle = \langle b|H|a\rangle^*$ , and  $\langle b|H|b\rangle$  using the form of the Hamiltonian as in Eq. (3.31). To simplify the description, I shall write the total Hamiltonian as a sum of two operators:

$$\hat{H} = \hat{T} + \hat{H}_C, \quad (3.57)$$

where  $\hat{T}$  is the single-particle energy operator, describing the motion of each particle in the external confinement of the nanostructure, and  $\hat{H}_C$  is the Coulomb operator. I shall calculate the matrix elements of each of these two operators separately.

### Single-particle energy operator

The single-particle energy operator written using the Fock-Darwin creation and annihilation operators takes the form:

$$\hat{T} = \sum_{nm\sigma} E(n, m, \sigma) c_{nm\sigma}^+ c_{nm\sigma}. \quad (3.58)$$

Let us calculate in detail the matrix element  $T_{aa} = \langle a|\hat{T}|a\rangle$ .

$$T_{aa} = \sum_{nm\sigma} E(n, m, \sigma) \langle 0|c_{0,0,\uparrow}c_{0,1,\downarrow}c_{0,0,\downarrow}|c_{nm\sigma}^+c_{nm\sigma}|c_{0,0,\downarrow}^+c_{0,1,\downarrow}^+c_{0,0,\uparrow}^+|0\rangle. \quad (3.59)$$

This matrix element has a form of a sum over the single-particle indices  $nm\sigma$ . Note that the operator  $c_{nm\sigma}^+c_{nm\sigma} = n_{nm\sigma}$  is a number operator, returning the number of electrons on the orbital  $nm\sigma$ . Therefore the only nonzero terms in this sum will be those with the

indices  $nm\sigma$  corresponding to the indices of one of the creation operators in the state  $|a\rangle$ ; other orbitals contain zero electrons. Therefore, in this case

$$\begin{aligned} T_{aa} &= E(0, 0, \downarrow) \langle 0 | c_{0,0,\uparrow} c_{0,1,\downarrow} c_{0,0,\downarrow} | n_{0,0,\downarrow} c_{0,0,\downarrow}^+ c_{0,1,\downarrow}^+ c_{0,0,\uparrow}^+ | 0 \rangle \\ &+ E(0, 1, \downarrow) \langle 0 | c_{0,0,\uparrow} c_{0,1,\downarrow} c_{0,0,\downarrow} | n_{0,1,\downarrow} c_{0,0,\downarrow}^+ c_{0,1,\downarrow}^+ c_{0,0,\uparrow}^+ | 0 \rangle \\ &+ E(0, 0, \uparrow) \langle 0 | c_{0,0,\uparrow} c_{0,1,\downarrow} c_{0,0,\downarrow} | n_{0,0,\uparrow} c_{0,0,\downarrow}^+ c_{0,1,\downarrow}^+ c_{0,0,\uparrow}^+ | 0 \rangle. \end{aligned} \quad (3.60)$$

Since in each case the orbitals defined by the indices of the number operator contain one electron, all expectation values of  $\hat{n}$  will be equal to 1, and the matrix element

$$T_{aa} = E(0, 0, \downarrow) + E(0, 1, \downarrow) + E(0, 0, \uparrow). \quad (3.61)$$

Thus, the matrix element  $T_{aa}$  is equal to the sum of the single-particle energies of orbitals occupied by each electron. Similarly one can show that

$$T_{bb} = E(0, 1, \downarrow) + E(1, 0, \downarrow) + E(0, 1, \uparrow). \quad (3.62)$$

The off-diagonal matrix elements  $\langle a | \hat{T} | b \rangle = \langle b | \hat{T} | a \rangle$  involve expectation values of the type  $\langle a | n_{nm\sigma} | b \rangle$ . Since the number operator  $\hat{n}$  cannot redistribute electrons, these expectation values will be zero. Thus, the single-particle energy operator in my basis is a diagonal matrix:

$$\hat{T} = \begin{bmatrix} T_{aa} & 0 \\ 0 & T_{bb} \end{bmatrix}. \quad (3.63)$$

Note that if the configurations are built out of the Hartree-Fock orbitals instead of the Fock-Darwin ones, this operator can contain nonzero off-diagonal elements, as can be seen from the form of the operator  $\hat{T}$  in Eq. (3.38).

### Coulomb operator

Let us now focus on the Coulomb operator

$$\hat{H}_C = \frac{1}{2} \sum_{ijkl} \langle ij | v | kl \rangle c_i^+ c_j^+ c_k c_l, \quad (3.64)$$

where the composite index  $i = nm\sigma$ ; the same applies to  $j$ ,  $k$ , and  $l$ . In what follows I shall make use of the fact that my single-particle basis set is ordered according to the spin and single-particle energy, so, for instance, the notation  $k > l$  will mean that the orbital  $k$  is higher up in the single-particle basis than the orbital  $l$ .

In the Coulomb operator (3.64) the composite indices run over all available single-particle orbitals. In particular, I need to consider terms with  $k < l$  and  $k > l$  (the term with  $k = l$  is identically zero, since in this case the two annihilation operators would act on the same orbital).

I shall now demonstrate that I can reduce the number of terms in the sum in Eq. (3.64) using the Fermionic commutation rules for the operators  $c$  and  $c^+$  written in Eq. (3.4).

Let us focus on the indices  $k$  and  $l$  first. I can separate the sum into two terms: one for  $k < l$ , and one for  $k > l$ :

$$\hat{H}_C = \frac{1}{2} \left( \sum_{i,j,k < l} \langle ij|v|kl \rangle c_i^+ c_j^+ c_k c_l + \sum_{i,j,k > l} \langle ij|v|kl \rangle c_i^+ c_j^+ c_k c_l \right). \quad (3.65)$$

In the second term I interchange the two annihilation operators, observing the Fermionic commutation rules:  $c_k c_l = -c_l c_k$ . I also rename the dummy indices:  $k \rightarrow l$  and  $l \rightarrow k$ . This allows me to write the Coulomb operator in the form:

$$\hat{H}_C = \frac{1}{2} \sum_{i,j,k < l} (\langle ij|v|kl \rangle - \langle ij|v|lk \rangle) c_i^+ c_j^+ c_k c_l. \quad (3.66)$$

The first term in this sum is the Coulomb direct element. This matrix element attains a nonzero value only if the spin of the orbital  $|i\rangle$  is the same as that of the orbital  $|l\rangle$  and the spin of the orbital  $|j\rangle$  is the same as that of the orbital  $|k\rangle$ , however, the spin of  $|i\rangle$  can be different than that of  $|j\rangle$ . The second term in the sum is the Coulomb exchange element. This matrix element attains a nonzero value only if the scattered particles have the same spin.

I can perform a similar simplification for orbitals  $i$  and  $j$ . As a result, I will obtain another pair of matrix elements, one direct and one exchange, identical to the elements in Eq. (3.66). Upon their summation the factor 1/2 in front of the sum is eliminated, and

the final form of the Coulomb operator is

$$\hat{H}_C = \sum_{i>j,k<l} (\langle ij|v|kl\rangle - \langle ij|v|lk\rangle) c_i^+ c_j^+ c_k c_l. \quad (3.67)$$

Let us now calculate the matrix elements of the Coulomb operator  $\hat{H}_C$  in my basis  $\{|a\rangle, |b\rangle\}$  of the three-electron configurations, starting with the diagonal element  $\langle a|\hat{H}_C|a\rangle = H_C^{aa}$ .

$$H_C^{aa} = \sum_{i>j,k<l} (\langle ij|v|kl\rangle - \langle ij|v|lk\rangle) \langle 0|c_{0,0,\uparrow}c_{0,1,\downarrow}c_{0,0,\downarrow}|c_i^+c_j^+c_k c_l|c_{0,0,\downarrow}^+c_{0,1,\downarrow}^+c_{0,0,\uparrow}^+|0\rangle. \quad (3.68)$$

Note that the element  $\langle 0|c_{0,0,\uparrow}c_{0,1,\downarrow}c_{0,0,\downarrow}|c_i^+c_j^+c_k c_l|c_{0,0,\downarrow}^+c_{0,1,\downarrow}^+c_{0,0,\uparrow}^+|0\rangle$  can be understood as the dot product of two vectors:

$$c_j c_i c_{0,0,\downarrow}^+ c_{0,1,\downarrow}^+ c_{0,0,\uparrow}^+ |0\rangle \quad \text{and} \quad c_k c_l c_{0,0,\downarrow}^+ c_{0,1,\downarrow}^+ c_{0,0,\uparrow}^+ |0\rangle, \quad (3.69)$$

with  $i > j$  and  $k < l$ . It is now clear why I chose these boundaries in summation in Eq. (3.67): in each case, out of the two annihilation operators, the first one (i.e.,  $c_i$  and  $c_l$ , respectively) removes an electron created deeper (farther to the right) in the sequence of operators  $c^+$  as compared to the second annihilation operator (i.e.,  $c_j$  and  $c_k$ , respectively). This simplifies the automatic computation of the matrix elements, since I do not have to check whether a given electron in the configuration has already been removed or not.

Let us now enumerate the possible sets of orbitals  $i, j$  and  $k, l$ , for which the vectors in Eq. (3.69) are nonzero. As for the pair  $i, j$ , there are three possibilities. One of them is  $i = (0, 1, \downarrow)$ ,  $j = (0, 0, \downarrow)$ , which gives

$$c_{0,0,\downarrow}c_{0,1,\downarrow}c_{0,0,\downarrow}^+c_{0,1,\downarrow}^+c_{0,0,\uparrow}^+|0\rangle = -c_{0,0,\uparrow}^+|0\rangle.$$

The minus sign in the above expression is a phase factor, originating from the fact that in order to act with the operator  $c_{0,1,\downarrow}$ , I need to reverse the order of this operator and the first creation operator in the sequence. This introduces the minus sign due to the Fermionic commutation rules of these operators.

The second possible pair of orbitals  $i, j$  is  $i = (0, 0, \uparrow)$ ,  $j = (0, 0, \downarrow)$ ; upon their application I am left with the vector  $+c_{0,1,\downarrow}^+|0\rangle$ . Here the phase factor is positive because in order to act with  $c_{0,0,\uparrow}$ , I need to reverse the order of operators twice.

Finally, the third possible pair of orbitals is  $i = (0, 0, \uparrow)$ ,  $j = (0, 1, \downarrow)$ . Their application gives  $-c_{0,0,\downarrow}^+|0\rangle$ , the negative phase being due to the three reversals of operators necessary to complete it.

Since the second vector in Eq. (3.69) is exactly the same as the first one, the possible pairs of orbitals  $k, l$  are identical to the pairs  $i, j$  described above. This gives  $3 \times 3 = 9$  possible terms in the sum (3.68). The number of terms is further decreased by considering the dot products of the vectors from Eq. (3.69) for each combination of orbitals. These dot products will be nonzero only if the third electron (i.e., the electron that remains after the application of annihilation operators) is the same on either side. In the case of diagonal matrix elements of the Coulomb operator, and in particular for the element  $H_C^{aa}$ , this happens only if the orbitals  $i = l$  and  $j = k$ . Thus the number of nonzero dot products is reduced to three, and the matrix element

$$\begin{aligned} H_C^{aa} &= (\langle 01, 00|v|00, 01\rangle - \langle 01, 00|v|01, 00\rangle) \\ &+ \langle 00, 00|v|00, 00\rangle + \langle 00, 01|v|01, 00\rangle. \end{aligned} \quad (3.70)$$

The term in braces corresponds to the orbitals  $i = l = (0, 1, \downarrow)$ ,  $j = k = (0, 0, \downarrow)$  and consists of the direct and exchange elements because the scattered electrons have the same spins. The two remaining terms in  $\hat{H}_C^{aa}$  correspond to the two other sets of orbitals and consist of direct elements only.

In an analogous fashion one can show that the second diagonal matrix element of the Coulomb operator is

$$\begin{aligned} H_C^{bb} &= (\langle 10, 01|v|01, 10\rangle - \langle 10, 01|v|10, 01\rangle) \\ &+ \langle 01, 01|v|01, 01\rangle + \langle 01, 10|v|10, 01\rangle. \end{aligned} \quad (3.71)$$

The off-diagonal matrix element  $\hat{H}_C^{ab}$ , on the other hand, consists of only one term:

$$H_C^{ab} = -\langle 00, 00|v|10, 01\rangle. \quad (3.72)$$

This term corresponds to the following choice of orbitals:  $i = (0, 0, \uparrow)$ ,  $j = (0, 0, \downarrow)$ ,  $k = (1, 0, \downarrow)$ ,  $l = (0, 1, \uparrow)$ . It has a negative phase, because the application of operators  $c_j c_i$  requires two interchanges of operators, and application of the pair  $c_k c_l$  requires three such interchanges. Thus the phase is  $(-1)^{2+3} = (-1)$ .

### The full Hamiltonian

I am now ready to write my full Hamiltonian matrix in the basis  $\{|a\rangle, |b\rangle\}$ :

$$\hat{H} = \begin{bmatrix} T_{aa} + H_C^{aa} & H_C^{ab} \\ (H_C^{ab})^* & T_{bb} + H_C^{bb} \end{bmatrix}. \quad (3.73)$$

If I calculate the elements of the single-particle energy operator using the Fock-Darwin energies, and the elements of the Coulomb operator using the matrix elements  $\langle ij|v|kl\rangle$  in the harmonic-oscillator basis, the resulting Hamiltonian matrix takes the form:

$$\hat{H} = \begin{bmatrix} \frac{3}{2}\hbar\omega_+ + \frac{5}{2}\hbar\omega_- + 2.25E_0 & -0.25E_0 \\ -0.25E_0 & \frac{5}{2}\hbar\omega_+ + \frac{7}{2}\hbar\omega_- + 1.875E_0 \end{bmatrix}, \quad (3.74)$$

where  $E_0 = \sqrt{\pi}/\ell$ . The eigenvalues of this simple matrix can be obtained analytically, and are

$$E_1 = 2\hbar\omega_+ + 3\hbar\omega_- + 2.0625E_0 + \frac{\sqrt{(\hbar\omega_+ + \hbar\omega_- - 0.375E_0)^2 + 0.25E_0^2}}{2}, \quad (3.75)$$

$$E_2 = 2\hbar\omega_+ + 3\hbar\omega_- + 2.0625E_0 - \frac{\sqrt{(\hbar\omega_+ + \hbar\omega_- - 0.375E_0)^2 + 0.25E_0^2}}{2}. \quad (3.76)$$

In this model calculation I assumed a very simple, two-element basis set. Later on I shall use much larger basis sets of configurations, however in all such cases the rules of constructing the Hamiltonian matrix remain the same.

The last step of the exact diagonalisation approach involves numerical diagonalisation of the Hamiltonian matrix. To this end I could use the numerical procedures appropriate

for full matrices, requiring that the entire matrix be stored in the memory of the computer. This, however, would be limiting, since the matrix of order of about  $11000 \times 11000$  with elements encoded using 8-byte numbers (standard double-precision format) occupies about 1 gigabyte of memory; I would be thus restricted to the sizes of the basis set no larger than a few tens of thousands. I am, however, interested in much larger bases, composed of millions of configurations. Processing of such large Hamiltonian matrices can be accomplished only by exploiting the fact that they are *sparse*.

A matrix is sparse if the majority of its off-diagonal matrix elements is equal to zero. In my Hamiltonian the off-diagonal elements can only be due to the Coulomb operator. This operator has two important properties: each term in the sum (3.67) has to conserve the angular momentum of the scattered pair of electrons, and the dot product of the two vectors obtained after the application of operators  $c_j c_i$  and  $c_k c_l$  has to be nonzero. These properties impose stringent conditions on the pairs of vectors that can be coupled by  $\hat{H}_C$ , and lead to vanishing of typically about 80% of off-diagonal elements. Thus my Hamiltonian matrix is typically sparse, and I can save the computer memory by storing only its nonzero elements. This, however, prevents me from using the most popular linear algebra packages, such as LAPACK [71], since they are not compatible with such a packed matrix storage. Therefore I need to develop a numerical diagonalisation algorithm which is designed specifically to handle sparse matrices. I describe two such algorithms in the next Section.

### 3.3.4 Diagonalisation of large and sparse matrices

In the previous Section I have shown how I can decrease the size of the many-particle basis of configurations of  $N$  electrons distributed on  $M$  single-particle levels by accounting for the symmetries of the system. But the accuracy of the results of the configuration-interaction method is still affected by the choice of the cutoff  $M$  chosen to limit the number of single-particle orbitals: in order to obtain reliable results, the number  $M$

should be as large as possible. Therefore, by exploiting the symmetries of the system I have not eliminated the problem of large matrices; I just replaced them by ones, whose diagonalisation will yield results which are much more accurate than those obtained using the unoptimised basis set of the same size. These matrices still have sizes at least of  $10^5 \times 10^5$ , and special techniques must be used to diagonalise them. In my research I employ the iterative conjugate gradient method combined with spectrum folding. I shall describe these techniques in this Section.

In discussing the conjugate gradient method of matrix diagonalisation I shall first focus on a simpler technique - the steepest descent method - in which the entire principle of iterative minimisation is not obscured by optimisation details. I will assume that the Hamiltonian matrix  $H$  is real and symmetric, which guarantees real eigenvalues. This applies directly to the many-body problem, since the many-body Hamiltonian matrix is real in the basis of configurations. The method can, however, be easily generalised to treat complex Hermitian matrices as well.

Both the steepest descent and the conjugate gradient methods are of iterative nature, and their general premise is to “generate” a guess vector and then “purify” it according to some algorithm. This purification process aims at obtaining the exact eigenvector corresponding to the *lowest eigenvalue* of  $H$ . The process is executed with the constraint that the vector being processed be normalised to 1.

The steepest descent and conjugate gradient methods presented here are special cases of the general steepest descent and conjugate gradient methods, which deal with finding a minimum of a multivariable function. The only thing that makes them special is the normalisation constraint mentioned before. The general methods are constructed with the assumption that the user supplies the multidimensional function  $f(x_1, x_2, \dots, x_N)$  to be minimised. The first step is to generate a random starting point (the “guess vector”)  $\vec{u}_0 = [x_1^{(0)}, x_2^{(0)}, \dots, x_N^{(0)}]$ , whose coordinates are chosen using a random number generator. This point, in general, is away from the minimum of the function  $f$ . Now I calculate the



gradient of the function  $f$  at the point  $\vec{u}_0$ :

$$\nabla f(\vec{u})|_{\vec{u}=\vec{u}_0} = \left[ \frac{\partial f}{\partial x_1}, \frac{\partial f}{\partial x_2}, \dots, \frac{\partial f}{\partial x_N} \right] \Big|_{\vec{u}=\vec{u}_0}. \quad (3.77)$$

This vector shows the direction of the steepest increase of the function, and the vector  $-\nabla f(\vec{u})|_{\vec{u}=\vec{u}_0}$  shows the direction of the steepest descent. I can then take a step of some length from the point  $\vec{u}_0$  along the direction of the steepest descent, and this hopefully will shift me closer to the global (or local) minimum of the function  $f$ . At the new point,  $\vec{u}_1$ , I do the same, i.e., calculate the direction of the steepest descent and take the next step. I expect that after a sufficiently large number of steps I will descend to the actual minimum of  $f$ . This is the method of the steepest descent.

Sophisticated methods have been developed to calculate the desirable length of the step mentioned above. Also, sometimes steps are taken not along the direction of the steepest descent, but along a set of “conjugate” directions. The idea of “conjugacy” involves creating the next direction of the step based not only on the gradient, but also on previous step directions. In this way one never steps along the same direction twice.

To better visualise these techniques, let us consider a simple two-dimensional problem of a long and deep potential valley. My goal is to find the lowest point (minimum) in this valley, but for now without any normalisation constraints. If I choose a random starting point, say, on one of the walls of the valley, and then take a step along the direction of steepest descent, I may end up somewhere on the opposite wall of this valley. If the shape of the potential valley is strongly asymmetric (the valley is very long and narrow), in the next iteration I may return close to the starting point (the subsequent directions of steepest descent will be nearly parallel). I will, most likely, ultimately find a minimum, but this convergence can take place after a large number of steps. I can limit the number of steps taken in the steepest descent procedure by imposing additional requirements on subsequent directions in which I step - make them conjugate. In such procedure, the first step is always taken along the direction of steepest descent. However, if my function  $f$  depends only on two variables, it is possible to construct a conjugate direction that

already in the second step of the iteration will take me directly to the minimum of the function if the function is a quadratic polynomial, or very close to the minimum, if the function is more complicated. For a detailed description of the general steepest descent and conjugate gradient methods I refer the reader to Ref. [109].

Now I set out to adopt the technique described above to find the lowest eigenvalue of the matrix  $H$ . To this end I define my function  $f$  as the expectation value of the Hamiltonian in the state  $|u\rangle$ :

$$f(\vec{u}) = \langle u|H|u\rangle, \quad (3.78)$$

where  $|u\rangle = \vec{u} = [x_1, x_2, \dots, x_N]$ . This vector is understood as a shorthand notation of a many-particle state of the system. This state is a linear combination of many-particle configurations, from which I constructed my basis set. To make the notation compact, I simply retain the coefficients that correspond to each configuration in this combination. Here I also assumed that the size of the basis, and the dimension of the Hamiltonian  $H$ , is  $N$  (in this Section, this symbol does not denote the number of electrons).

Therefore, I have a function of  $N$  variables, defined as an expectation value of the Hamiltonian  $H$ , but with the normalisation constraint:  $\langle u|u\rangle = x_1^2 + x_2^2 + \dots + x_N^2 = 1$ . The above function is a long sum of terms such as  $u_i u_j H_{kl}$ , so if it was not for the constraint, it would be a quadratic function in the variables (a quadratic form). The additional constraint complicates the picture, since one of the variables becomes dependent on all other variables, and can be eliminated from the function  $f$ . However, in this approach I shall not carry out this elimination explicitly. I will only be interested in finding the set of variables  $x_1, x_2, \dots, x_N$  giving the smallest possible value of the function  $f$ , while still fulfilling the normalisation condition. Note that the minimum thus found does not necessarily correspond to the unconstrained global minimum of the function  $f$ . It is rather a *conditional* minimum of  $f$ , the condition being, of course, the normalisation. Thus, as an output from this method I shall obtain the smallest eigenvalue of the matrix  $H$ , and the corresponding eigenvector, and I have reduced the diagonalisation problem to the

minimisation of a function  $f$ .

The reader will find a detailed review of methods, by means of which this problem can be solved, in Ref. [95]. In this article, Payne *et al.* describe a wide variety of techniques, including molecular dynamics, Car-Parinello techniques, etc. Among them I also find the steepest descend and conjugate gradient approaches, however, Payne *et al.* give only a general description of principles on which these methods operate. The specific algorithm presented in detail in this Section has been created and implemented by the author of this Thesis.

I have chosen these two methods for an important reason. As I mentioned in the previous Section, the sizes of Hamiltonian matrices that I typically encounter are of order of hundreds of thousands, and it is not possible to store these matrices in full form in computer memory. The two iterative methods are designed to circumvent this obstacle: they do not require the full matrix  $H$  as input, but rather the result of the matrix-vector multiplication. This gives the user a great flexibility in the choice of matrix storage mechanism: the user can store only nonzero matrix elements, use some symmetries of the matrix  $H$  characteristic for the problem at hand, or even calculate the matrix elements on the fly. The fundamental object being processed in each method is the vector itself, and one needs to provide a workspace consisting of several such vectors. Therefore, one never handles the object of the size of  $N \times N$ , only a few objects of the size of  $N$ . Unfortunately, this great advantage comes at a cost: the methods can only calculate one - the lowest - eigenvalue of the matrix at a time. To obtain other eigenvalues and eigenvectors one needs to employ additional techniques, such as reorthogonalisation. Later on in this Section I shall describe one such technique - the spectrum folding method, which is very stable numerically and simple to implement.

Let us start the presentation with the description of the **steepest descent method**. Below I shall enumerate the steps which must be taken in the iterative procedure.

1. As mentioned before, I start with a guess vector  $|u\rangle_0$ . This vector is generated at

random, and *should not* be initialised by assigning identical values to all its entries. This is because in doing so one might accidentally impose a symmetry on the vector which is different from the symmetry of the actual eigenvector corresponding to the lowest eigenvalue. In such situation the procedure might converge to one of the excited states, which is uncontrollable, and thus discouraged. One cannot count on this phenomenon as a possible way of implementing the finding of the excited states, because the imposed symmetry can be broken due to the buildup of the computational error incurred in each iteration. The vector generated at random will, on the other hand, contain elements of all possible symmetries, and it will be possible to purify it to the symmetry of the ground state.

Once initialised, the guess vector  $|u\rangle_0$  should be normalised to 1, so that  $\langle u|u\rangle = 1$ . Now I can calculate the first value of my function:  $E_0 = f(|u\rangle_0) = {}_0\langle u|H|u\rangle_0$ .

2. Now I need to find the direction of steepest descent. To this end let us make an explicit use of the fact that the vector  $|u\rangle$  must be normalised to 1 at each step of iteration. Therefore, the next approximation of the eigenvector can be achieved only by a rotation of the current vector by a certain angle, i.e.,

$$|u\rangle_1 = \cos(\alpha)|u\rangle_0 + \sin(\alpha)|g\rangle_0, \quad (3.79)$$

where the auxiliary vector  $|g\rangle_0$  must be normalised to 1 and orthogonal to  $|u\rangle_0$ . This orthogonality is required, because without it I would change the norm of  $|u\rangle$ : if  $|g\rangle_0$  has a component parallel to  $|u\rangle_0$ , I would add some length to the vector  $|u\rangle_0$ , which must be avoided. To prove that, let us consider explicitly the normalisation:

$${}_1\langle u|u\rangle_1 = \cos^2(\alpha) {}_0\langle u|u\rangle_0 + \sin^2(\alpha) {}_0\langle g|g\rangle_0 + 2 \sin(\alpha) \cos(\alpha) {}_0\langle g|u\rangle_0. \quad (3.80)$$

The above norm equals 1 only if both vectors are normalised (from the first two terms I get  $\cos^2(\alpha) + \sin^2(\alpha) = 1$ ) and orthogonal (the third term vanishes). The angle  $\alpha$  will be defined afterwards, now I will focus on generating the vector  $|g\rangle_0$ .

Let us postulate it in the form:

$$|g\rangle_0 = (H - E_0 I)|u\rangle_0. \quad (3.81)$$

As defined above,  $E_0 = {}_0\langle u|H|u\rangle_0$  is the zeroth approximation to the sought energy, calculated with the guess vector  $|u\rangle_0$ , and  $I$  is the unit matrix. Now I shall prove that the vector  $|g\rangle_0$  is orthogonal to  $|u\rangle_0$ :

$${}_0\langle u|g\rangle_0 = {}_0\langle u|H - E_0 I|u\rangle_0 = {}_0\langle u|H|u\rangle_0 - E_0 {}_0\langle u|u\rangle_0 = E_0 - E_0 = 0, \quad (3.82)$$

from the definition of  $E_0$  and because the vector  $|u\rangle_0$  is normalised to 1.

Let us now use the vector  $|g\rangle_0$ , henceforth called “gradient”, to rotate the guess vector  $|u\rangle_0$ . I have shown how this is accomplished in Eq. (3.79); now I only have to define the angle  $\alpha$ . To do that, let us calculate the next approximation to the eigenvalue:

$$E_1(\alpha) = {}_1\langle u|H|u\rangle_1 = \cos^2(\alpha)E_0 + \sin^2(\alpha) {}_0\langle g|H|g\rangle_0 + 2 \sin(\alpha) \cos(\alpha) {}_0\langle g|H|u\rangle_0. \quad (3.83)$$

Note that all matrix-vector multiplications appearing in the above equation can be carried out explicitly, because the only unknown here is  $\alpha$ . I choose its value so that  $E_1(\alpha)$  is minimal, and I can do it analytically by calculating the derivative  $dE_1(\alpha)/d\alpha$  and equating it to zero. I obtain, after elementary calculations,

$$\tan(2\alpha) = \frac{2 {}_0\langle g|H|u\rangle_0}{E_0 - {}_0\langle g|H|g\rangle_0}; \quad \alpha = \frac{1}{2} \arctan \left( \frac{2 {}_0\langle g|H|u\rangle_0}{E_0 - {}_0\langle g|H|g\rangle_0} \right). \quad (3.84)$$

In reality the trigonometric equation  $dE_1(\alpha)/d\alpha = 0$  has two solutions in the domain  $0 \leq \alpha \leq 2\pi$ :  $\alpha$  as written above, and  $\alpha + \pi/2$ ; one solution corresponds to the maximum, and one - to the minimum. I do not know a priori which solution to take. I therefore need to calculate both  $E_1(\alpha)$  and  $E_1(\alpha + \pi/2)$  and compare them. The argument corresponding to the smaller value of  $E_1$  is taken for further calculations. Using this  $\alpha$  I can get the next approximation to the vector  $|u\rangle_1$  and the energy  $E_1$  explicitly.

The last step is to normalise  $|u\rangle_1$  manually. Of course, if all the steps described above were performed with infinite precision, this step would not be necessary. However, I deal with finite-precision calculations, and the machine error will accumulate with each iteration. I circumvent this problem by renormalising the vector  $|u\rangle_1$ .

3. I repeat the procedure described in item 2, only treating the vector  $|u\rangle_1$  and eigenvalue  $E_1$  as known, and using them to calculate the next vector,  $|u\rangle_2$ , and the next eigenvalue,  $E_2$ . I do so iteratively in a loop, until the relative difference between two consecutive approximations of the eigenvalue is smaller than the predefined accuracy factor:

$$\left| \frac{E_{i+1} - E_i}{E_i} \right| \leq EPS. \quad (3.85)$$

The value  $EPS$  is defined by the user, but it should not be smaller than the respective machine accuracy (typically  $10^{-16}$ ). Note that the user does not have to preset the number of iterations, which would decrease the generality of the method. The iterative procedure should be self-terminating - upon fulfilment of the accuracy condition (3.85).

Let us now move on to the optimised version of the steepest descent approach - the **conjugate gradient method**. The goal of the optimisation is to limit the number of iterations necessary to reach convergence. I shall attempt to accomplish this by influencing the choice of auxiliary vectors  $|g\rangle_i$  in each iteration. This will be, however, the only difference distinguishing this algorithm from the steepest descent method.

As described above, the directions generated in the steepest descent method are completely defined by the matrix  $H$  and the current vector  $|u\rangle_i$ , without any correlation with any previous gradients  $|g\rangle_j$  or vectors  $|u\rangle_j$  with  $j < i$ . In particular, the gradient in step  $i$ ,  $|g\rangle_i$ , does not have to be orthogonal to the gradient in the step  $j$ ,  $|g\rangle_j$ , which means that I will rotate the vector  $|u\rangle$  (at least partially) in the same direction in both steps. It would be best, however, not to repeat the rotation direction that has already been used.

The idea here is to orthogonalise the gradient vector in step  $i$ ,  $|g\rangle_i$ , to all the previous gradients, i.e. to define a *direction*  $|d\rangle_i$ , which is equal to the gradient  $|g\rangle_i$ , but with all previous gradients  $|g\rangle_j$  projected out of it. That way each new direction will be orthogonal to all previous ones, and I will never retrace the steps already taken. It can be proved, however, that the problem posed in this way is over-constrained [109]: the construction of a sequence of steps along these lines requires the prior knowledge of the solution, which I seek.

However, instead of enforcing *orthogonality* of directions, I can enforce their *conjugacy*. Two vectors,  $|x\rangle$  and  $|y\rangle$  are conjugate if they fulfill the condition

$$\langle x|H|y\rangle = 0. \quad (3.86)$$

(note that the orthogonality condition is  $\langle x|y\rangle = 0$  and does not involve the Hamiltonian matrix  $H$ ). As I shall describe, it is possible to create a set of conjugate vectors recursively, retaining in memory only two immediately preceding vectors (the generation of an orthogonal set requires knowledge of *all* previous vectors).

The procedure starts by simply taking the gradient  $|d\rangle_0 = |g\rangle_0$  as the zeroth direction. I use this gradient to establish the next approximation to the eigenvector and eigenvalue, precisely as it was done in the steepest descent method.

In the first step of the algorithm I already have two objects: the gradient  $|g\rangle_1$ , and the direction from the previous step  $|d\rangle_0$ , and I can use these two. The direction in this step,  $|d\rangle_1$  is written as

$$|d\rangle_1 = |g\rangle_1 + \beta_1 |d\rangle_0. \quad (3.87)$$

Note that the two vectors on the right-hand side of this equation are known; I only have to establish the value of the parameter  $\beta_1$ . I do it by requiring that  $|d\rangle_1$  be conjugate to the previous direction,  $|d\rangle_0$ :

$${}_0\langle d|H|d\rangle_1 = 0; \quad \beta_1 = -\frac{{}_0\langle d|H|g\rangle_1}{{}_0\langle d|H|d\rangle_0}. \quad (3.88)$$

Now I look for the next approximation of the eigenvector and the eigenvalue using the direction  $|d\rangle_1$  rather than the gradient  $|g\rangle_1$  itself.

In each next step of the algorithm I generate the new direction in an analogous way:

$$|d\rangle_i = |g\rangle_i + \beta_i |d\rangle_{i-1}. \quad (3.89)$$

Note that I only use the current gradient and the previous direction in this process. The parameter  $\beta_i$  is calculated by requiring that  $|d\rangle_i$  be conjugate to  $|d\rangle_{i-1}$ , and is

$$\beta_i = -\frac{{}_{i-1}\langle d|H|g\rangle_i}{{}_{i-1}\langle d|H|d\rangle_{i-1}}. \quad (3.90)$$

In the case of the general conjugate method, i.e., the one in which I do not require the normalisation of the guess vector, it can be proved [109] that by this construction each direction is conjugate not only to the immediately previous one, but to all previous directions. In the current algorithm, in order to maintain the normalisation constraint, I introduce a new element: at each step the direction  $|d\rangle_i$  is additionally manually orthogonalised to the previous vector  $|u\rangle_i$ , before the new vector  $|u\rangle_{i+1}$  is obtained. This is aimed at conserving the normalisation of  $|u\rangle$ , as was already explained for the steepest descent, but it upsets the conjugacy. The new direction  $|d\rangle_i$  will be conjugate to the previous direction, and nearly conjugate to the one before that, but the conjugacy with earlier directions will be preserved to a lesser and lesser degree. This is a drawback, since it leads only to a local improvement of the rate of convergence. However, the loss of conjugacy does not cause the algorithm to diverge, nor converge to a wrong value; the algorithm will simply converge slower, but always to the correct eigenvalue.

Having understood the idea of conjugacy I shall now formulate the minimisation algorithm that employs it.

1. First I generate the guess vector  $|u\rangle_0$  and normalise it to 1; I also calculate  $E_0$  as described above.
2. I find the gradient  $|g\rangle_0$ , normalise it, and using it I find the appropriate parameter



$\alpha$  as I did in the steepest descent algorithm. This parameter  $\alpha$  is then used to generate the next approximation  $|u\rangle_1$  and  $E_1$ .

3. This step is unique to the conjugate gradient algorithm. I generate the next gradient,  $|g\rangle_1 = H|u\rangle_1 - E_1|u\rangle_1$ , but I am not using it in the rotation of the vector. Instead, I use the direction  $|d\rangle_1^* = |g\rangle_1 + \beta_1|d\rangle_0$ , with the parameter  $\beta_1 = -\frac{\langle d|H|g\rangle_1}{\langle d|H|d\rangle_0}$ . In general, the vector  $|d\rangle_1^*$  generated this way will not be orthogonal to  $|u\rangle_1$ . In order to preserve the norm of my approximate eigenvector  $|u\rangle$ , I need to perform the orthogonalisation manually, e.g., by taking a single step of the well-known Gram-Schmidt orthogonalisation:  $|d\rangle_1 = |d\rangle_1^* - \frac{\langle u|d\rangle_1^*}{\langle u|u\rangle_1}|u\rangle_1$ . Of course, the above expression can be written in a simpler form - without the denominator, since the approximate eigenvector  $|u\rangle_1$  is normalised. If execution time is absolutely crucial, the denominator can then be simply set to 1, as it should be in theory. However, this may not be so in practice due to the computer roundoff errors.
4. Now that I have the old approximate vector  $|u\rangle_1$  and the new direction  $|d\rangle_1$ , I can generate the new approximate vector  $|u\rangle_2$  in precisely the same way as I did for the steepest descent - writing it as a rotation and calculating the appropriate angle  $\alpha$ . Thus I obtain  $|u\rangle_2$  and the corresponding approximate eigenvalue  $E_2$ .
5. I repeat the step 3 until the convergence is reached.

To compare the performance of the two algorithms, I take the model Hamiltonian matrix describing a two-dimensional quantum well with rigid walls, discretised on a mesh of points. The continuous Schrödinger equation in the effective Rydberg units takes here the form

$$\left[ -\frac{\partial^2}{\partial x^2} - \frac{\partial^2}{\partial y^2} \right] \phi(x, y) = E\phi(x, y), \quad (3.91)$$

where  $0 \leq x \leq 1$  and  $0 \leq y \leq 1$  (the length of the sides of the square well is equal 1  $a_B$ , and the walls are infinite). Elementary analytical calculations show that the ground-state energy in such a well is  $E_0 = 2\pi^2$  Rydbergs. The discretisation scheme involves replacing

the continuous function  $\phi(x, y)$  by the function  $\phi(x_i, y_j)$  defined on a mesh of discrete points. For the model calculation, let us assume that I have discretised the system in such a way that there are  $M + 2$  points along each wall of the well, numbered from 0 (the first point has number 0, the second - number 1, and so on, until the last,  $M + 2$ -nd point which has the number  $M + 1$ ). Therefore the distance between points along each coordinate axis is  $\Delta x = \Delta y = \frac{1}{M+1}$ . The first and last of the mesh points coincide with the wall of the well, and therefore I expect the wave function to be equal to zero on those points. The function may assume nonzero values only on the mesh inside the well, and this mesh comprises  $M^2$  points.

I also need to discretise the second derivatives in the Schrödinger equation:

$$\left. \frac{\partial^2}{\partial x^2} \phi(x, y) \right|_{x_i, y_j} \approx \frac{\phi(x_{i-1}, y_j) - 2\phi(x_i, y_j) + \phi(x_{i+1}, y_j)}{(\Delta x)^2}, \quad (3.92)$$

and similarly for the derivative over the coordinate  $y$ . Upon this discretisation, the continuous Schrödinger equation (3.91) can be written as a set of linear equations of the type

$$-\phi(x_{i-1}, y_j) - \phi(x_i, y_{j-1}) + 4\phi(x_i, y_j) - \phi(x_{i+1}, y_j) - \phi(x_i, y_{j+1}) = (\Delta x)^2 E \phi(x_i, y_j) \quad (3.93)$$

for each of the points in the mesh, i.e., for  $1 \leq i \leq M$  and  $1 \leq j \leq M$ . Whenever the above equation requires the value of the function  $\phi$  on any of the walls of the well (i.e., for  $i = 0$  or  $i = M + 1$  or  $j = 0$  or  $j = M + 1$ ), the value 0 is explicitly introduced instead. I also order the equations in such a way that in the first one I have  $i = j = 1$ , in the second -  $i = 2$  and  $j = 1$ , etc, until I reach  $i = M, j = 1$ . After that I begin again with  $i = 1$  but this time  $j = 2$ . I continue this sequence until I reach the equation with  $i = j = M$ .

Such a set of equations can be written in a matrix form, with a penta-diagonal matrix  $H$  of order  $M^2 \times M^2$ . All the diagonal elements of this matrix are equal to 4, and on the immediate upper and lower diagonal I put  $-1$ , except for each  $M + 1$ -st element along it, which is set to zero (this is due to the rigid wall of the well, positioned next to this point on the mesh). Also, this matrix possesses a remote upper- and lower-diagonal, filled with

values  $-1$ , beginning respectively in the  $M + 1$ -st column and the  $M + 1$ -st row. Upon diagonalisation of this matrix I obtain the eigenvalues  $\varepsilon$ , which can be converted to the values of energy by rescaling  $E = \varepsilon/(\Delta x)^2$ .

In these model calculations I assume  $M = 50$  so that the simple Hamiltonian is of the size  $2500 \times 2500$ . The target eigenvalue - the ground-state energy that I should obtain in the diagonalisation - is  $\varepsilon_0 = \frac{2\pi^2}{51 \times 51} = 0.0075890845$ . Of course, I should not expect to obtain this value exactly, as the factor  $2\pi^2$  in this formula corresponds to the true solution of the continuous equation (3.91).

The steepest descent method applied to the matrix  $H$  converged to the value of  $0.007586685051830517$  after 3392 iterations. The relative error  $EPS$ , as calculated in the algorithms, was decreasing systematically in the progress of the calculation, attaining the value of about  $7.16 \cdot 10^{-6}$  after first 500 iterations, about  $7.82 \cdot 10^{-9}$  after first 1000 iterations, and  $1.41 \cdot 10^{-11}$  after 2000 iterations. Thus I deal with a long convergence tail. As for the conjugate gradient applied to the same matrix, it converged to the value of  $0.007586685051823797$  after only 174 iterations. A comparison of relative errors  $EPS$  of both methods as a function of the number of iterations is shown in Fig. 3.1. Note that the line corresponding to the steepest descent method exhibits some oscillatory behaviour just before reaching the convergence. The line corresponding to the conjugate gradient method does exhibit such behaviour as well, but to a much smaller degree. This performance comparison shows clearly the superiority of the conjugate gradient method over the steepest descent. The latter converged after taking more steps than the order of the matrix itself, whereas the conjugate gradient method converged after the number of steps equal to about 7% of the order of the matrix.

Both the steepest descent and conjugate gradient methods are capable of finding the ground state eigenvector and eigenenergy only. The last issue that I need to address is the use of the iterative methods in finding not only the ground, but also the excited states of the system. To this end I employ a technique called the **spectrum folding**

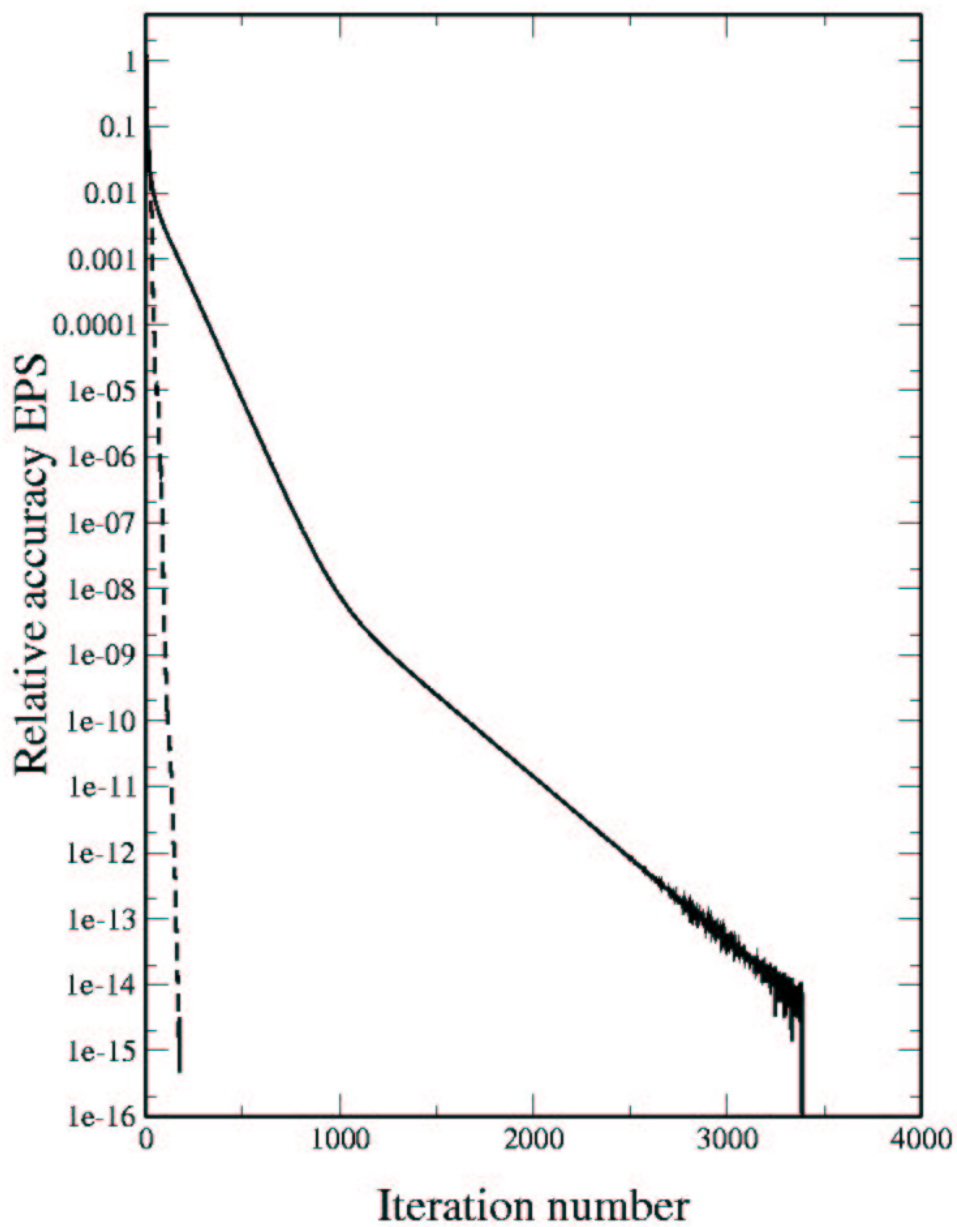


Figure 3.1: Relative error of the steepest descent (solid line) and the conjugate gradient (dashed line) methods as a function of the iteration number.

**method**, used extensively in large computations, e.g., by the group of Alex Zunger [28]. Preparation and implementation of the spectrum folding algorithm in the form described below, and coupling it with the conjugate gradient method is an original work of the author of this Thesis.

The spectrum folding method involves constructing a new Hamiltonian  $H_2$ , whose ground-state eigenvector is identical to the eigenvector corresponding to one of the excited states of the original Hamiltonian  $H$ . The new Hamiltonian is postulated in the form:

$$H_2 = (H - \varepsilon I)^2, \quad (3.94)$$

where  $\varepsilon$  is a user-supplied number with dimension of energy, and  $I$  is the unit matrix. Let us explain the meaning of the number  $\varepsilon$  later. First I shall look at the eigenvectors of  $H_2$ . Let us assume that the vector  $|v\rangle$  is one of the eigenvectors of the original Hamiltonian  $H$  with the eigenvalue  $E$ , i.e.,

$$H|v\rangle = E|v\rangle. \quad (3.95)$$

I have

$$H_2|v\rangle = (H - \varepsilon I)(H - \varepsilon I)|v\rangle = (E - \varepsilon)^2|v\rangle,$$

which means that the vector  $|v\rangle$  is also an eigenvector of  $H_2$ , but with eigenvalue  $(E - \varepsilon)^2$ . Thus, in transition from the Hamiltonian  $H$  to  $H_2$  the eigenvectors are unchanged, and the energies are transformed quadratically:  $E_i \rightarrow (E_i - \varepsilon)^2$ . To see what this gives me, let us assume for a moment that the original Hamiltonian  $H$  has both positive and negative eigenvalues, and let us take  $\varepsilon = 0$ . Clearly, upon transformation to the Hamiltonian  $H_2$  all the eigenvalues will be squared, so that all the negative eigenvalues will acquire the positive sign. Thus, by transforming  $H$  to  $H_2$ , I have parabolically “folded” the spectrum of the original Hamiltonian  $H$ . Note that the ground state of the Hamiltonian  $H_2$  will be *different* than the ground state of  $H$  - in fact, the ground state of  $H_2$  will be one of the excited states of  $H$ , the one, whose absolute value of eigenenergy was originally closest to zero. Now, if I tune the parameter  $\varepsilon$ , I can additionally shift the energy spectrum of  $H$ ,

which gives an ability to bring the eigenenergy of the chosen excited state of  $H$  to zero. This guarantees that the chosen excited state will become the ground state of  $H_2$ , and I can find it using the conjugate gradient algorithm. By appropriate tuning of  $\varepsilon$  I can thus find all the eigenstates of  $H$ , and the eigenenergies that correspond to them.

The last issue I shall address here is the choice of the most efficient way of tuning the shift  $\varepsilon$ . In principle, one could simply change it in some small steps over a chosen region of values. That would, however, require a long time, necessary to perform such a large number of iterative diagonalisations. There is also a danger that the eigenvalues of  $H$  can be clustered in such a way that the gaps between them are smaller than the step taken in tuning the shift  $\varepsilon$ ; such eigenvalues would be impossible to resolve with this procedure. To circumvent these obstacles, I propose a more efficient tuning scheme, involving partial reorthogonalisation of the guess vector. I proceed in the following way:

1. Find the ground-state eigenvector and eigenvalue of the original Hamiltonian  $H$ . To this end, I do not have to fold the spectrum, since the conjugate gradient method is constructed to find the lowest eigenvalues of matrices. The ground-state eigenvector found in this step is stored for further processing.
2. Find the *approximate* first-excited-state eigenvector and eigenvalue by performing the conjugate gradient minimisation with the original Hamiltonian  $H$ , but imposing an additional constraint on the guess vector  $|u\rangle$  in each iteration: not only does it have to be normalised, but also orthogonal to the ground-state eigenvector found and stored in the previous step. The orthogonalisation is accomplished by means of the Gram-Schmidt procedure.
3. Use the approximate eigenvalue of the first excited state - found in the previous step - as the shift  $\varepsilon$ . Use this shift to construct the Hamiltonian  $H_2$ , and perform the conjugate gradient procedure with it. The shift causes the first excited state of  $H$  to be the ground state of  $H_2$  with corresponding eigenvalue equal to zero. The

eigenvector found this way is stored for further processing.

4. Repeat steps 2 and 3 for higher and higher states of  $H$ , “guessing” the approximate eigenvalue corresponding to each of them by performing the conjugate-gradient minimisation with reorthogonalisation to all eigenstates previously found, and use this approximate eigenvalue as the shift in  $H_2$ . The reorthogonalisation procedure is not used in this step.

Note that this shifting-and-reorthogonalisation procedure allows to resolve even those eigenstates of  $H$ , whose eigenvalues are degenerate. Unfortunately, I pay for this functionality by extended storage requirements - I need to store all the eigenvectors found in subsequent steps. This may make it impossible to find *all* the eigenvalues and eigenvectors of  $H$ , but in my calculations I will be interested in resolving only the ground and several excited states of the system anyway. The most important feature of the proposed method is the fact that the numerical error, accumulating in the reorthogonalisation, *does not affect* the eigenvalues, since the reorthogonalisation steps are taken only in evaluating the optimal shift, and not the final result.

### 3.4 Other methods accounting for electronic correlations

In this Chapter I have built the optimised exact diagonalisation technique for many-body systems confined in QD potentials, and I have demonstrated its operation on a system of several interacting electrons confined in a two-dimensional parabolic potential. As I have shown, this method involves building a basis set out of electronic configurations, constructing the Hamiltonian matrix in this basis and diagonalising it numerically. This approach treats all aspects of the Coulomb interaction on equal footing (without any approximations), and therefore the results it gives are, in principle, *exact*. However, as I

have shown, the basis of many-particle configurations in a parabolic confinement is infinite, and, to be able to perform computations, I need to restrict it by considering only a finite number  $M$  of single-particle states, on which I distribute my electrons. This is, in fact, the only approximation of this method, and I can control it by performing convergence studies, in which I examine the ground-state energies of the system as a function of the parameter  $M$ . In Section 3.3 I have shown that even with the cutoff the number of electronic configurations necessary to obtain a well-converged result increases factorially both with the number of electrons  $N$  and the number of single-particle states  $M$ . This makes the method extremely unwieldy for larger electron numbers; using present-day computers I was only able to treat at most nine interacting particles.

But often of interest are properties of larger systems, and in these cases the configuration-interaction method can only be used to form general intuitions about their properties, as the limitation of the basis to manageable sizes prevents me from reaching convergence. In these cases other - approximate - methods must be used. Here I shall briefly describe two of such methods - the spin density functional theory (SDFT) and the quantum diffusion Monte Carlo method (QDMC) - which are also capable of resolving correlation effects, albeit in an approximate manner. The main point of this presentation is the fact that the results obtained with these methods can be compared to those of the exact diagonalisation for systems in which the performance of the latter technique is adequate. This allows to control the approximations made in SDFT and QDMC, so that, when these methods are applied to larger systems, their results are more reliable.

My description of SDFT and QMC methods will be limited to fundamentals only, as I shall not use them in the rest of this work. My goal here is to inform the reader of their existence and provide the appropriate literature context.



### 3.4.1 Spin density functional theory

In this Section I shall describe the fundamentals of the spin density functional theory. This description will be based on original papers of the contributors to this theory, but the reader can find excellent reviews of the subject in Refs. [116, 127]. To ensure consistency I shall use the notation proposed in these publications.

The development of the density functional theory (DFT) was started by P. Hohenberg and W. Kohn in 1964, who proved [60] that the energy of a system of interacting particles in an external potential is a unique functional of electronic density. In their work they introduced the following notation:

$$\hat{T} = -\frac{\hbar^2}{2m^*} \int d\mathbf{r} \Psi^+(\mathbf{r}) \Delta \Psi(\mathbf{r}); \quad (3.96)$$

$$\hat{V} = \int d\mathbf{r} V(\mathbf{r}) \Psi^+(\mathbf{r}) \Psi(\mathbf{r}); \quad (3.97)$$

$$\hat{W} = \frac{1}{2} \frac{e^2}{\varepsilon} \int d\mathbf{r} \int d\mathbf{r}' \frac{1}{|\mathbf{r} - \mathbf{r}'|} \Psi^+(\mathbf{r}) \Psi^+(\mathbf{r}') \Psi(\mathbf{r}') \Psi(\mathbf{r}). \quad (3.98)$$

Here,  $\hat{T}$  is the kinetic energy operator,  $\hat{V}$  is the operator introducing the external potential  $V(\mathbf{r})$ ,  $\hat{W}$  is the operator introducing the Coulomb interactions. The Hamiltonian of the system can be written as a sum of all these operators:

$$\hat{H} = \hat{T} + \hat{V} + \hat{W}. \quad (3.99)$$

Moreover,  $\Psi(\mathbf{r})$  are the field operators; with their use the electronic density operator can be written as

$$\hat{n}(\mathbf{r}) = \Psi^+(\mathbf{r}) \Psi(\mathbf{r}). \quad (3.100)$$

The Hohenberg-Kohn formalism treats the electronic density  $n(\mathbf{r})$  as the central quantity, by means of which all properties of the system can be described completely. In fact, even the electronic wave functions  $|\Psi[n]\rangle$  are functionals of the density. Now, the expectation value of any observable  $\hat{O}$  can be expressed as  $O = \langle \Psi[n] | \hat{O} | \Psi[n] \rangle$ , and, in particular, the energy

$$E[n] = \langle \Psi[n] | \hat{H} | \Psi[n] \rangle \quad (3.101)$$

is a unique functional of density. This *exact* result is the Hohenberg-Kohn theorem.

The formula for energy as a functional of the electronic density can be used to find the ground-state energy  $E_{GS}$  of the system. Hohenberg and Kohn prove that  $E_{GS} = E[n_0(\mathbf{r})]$  if the density  $n_0(\mathbf{r})$  fulfils two conditions: first, it minimises the functional  $E[n]$ , and second, it is normalised to give

$$N[n] = \int d\mathbf{r}n(\mathbf{r}) = N, \quad (3.102)$$

where  $N$  is the number of electrons in the system. The greatest strength of the Hohenberg-Kohn theorem is the fact that it allows to work with a three-dimensional electronic density instead of the  $3N$ -dimensional electronic wave function. As I shall show, this allows to treat electronic systems far larger than those treatable by the exact diagonalisation method provided that one is able to correctly minimise the energy functional for these systems.

In treating the electronic density up to now I have neglected the spin degree of freedom. This quantum number is, however, essential for systems of interest, as I have already demonstrated in Section 3.3.2. The inclusion of electronic spin into the DFT formalism in early 1970s led to the development of the spin density functional theory (SDFT) [13, 100]. In SDFT, the electronic density  $n(\mathbf{r})$  is replaced by a pair of densities,  $n_\uparrow(\mathbf{r})$  and  $n_\downarrow(\mathbf{r})$ , corresponding to electrons spin up and spin down, respectively. Therefore the field operators  $\Psi$  acquire an additional index, and are denoted as  $\Psi_\sigma(\mathbf{r})$ , and in the definitions (3.96), (3.97), (3.98) of energy operators the integration over coordinates must be supplemented by the summation over spins. Now the total energy of the system is a functional of the two densities,

$$E[n_\uparrow, n_\downarrow] = \langle \Psi[n_\uparrow, n_\downarrow] | \hat{H} | \Psi[n_\uparrow, n_\downarrow] \rangle, \quad (3.103)$$

and the ground state energy  $E_{GS}[n_\uparrow, n_\downarrow]$  can be obtained by minimising the above functional with respect to both densities under constraints

$$\int d\mathbf{r}n_\uparrow(\mathbf{r}) = N_\uparrow, \quad (3.104)$$

$$\int d\mathbf{r} n_{\downarrow}(\mathbf{r}) = N_{\downarrow}, \quad (3.105)$$

$$N_{\uparrow} + N_{\downarrow} = N, \quad (3.106)$$

where  $N_{\uparrow}$  ( $N_{\downarrow}$ ) is the number of electrons spin up (down).

The latest density-functional theories include an additional term in the Hamiltonian, accounting for the interaction of currents, created by orbiting electrons, with the magnetic field. This is the so-called current-spin density functional theory, developed by Vignale and Rasolt [125]. However, the current corrections - at least in the quantum-dot systems - have been shown to be very small [116, 127], and I shall not describe them further.

I have defined the object on which I need to work: the total energy as a functional of the electronic densities. Let us now briefly describe the minimisation procedure of this functional, used to obtain the ground state energy and density of the system. This procedure was developed by W. Kohn and L. Sham in 1965 [67]. To simplify the description, let us follow their notation and drop the spin index in densities and functionals; all the derivations presented below can be naturally extended to resolve the spin degree of freedom. To arrive at the famous Kohn-Sham equations, let us introduce an additional density functional

$$F[n] = \langle \Psi[n] | \hat{T} + \hat{W} | \Psi[n] \rangle, \quad (3.107)$$

being the expectation value of the Hamiltonian without the external potential  $\hat{V}$ . It is further convenient to isolate the so-called exchange-correlation energy:

$$E_{XC}[n] = F[n] - T[n] - \frac{1}{2} \frac{e^2}{\epsilon} \int d\mathbf{r} \int d\mathbf{r}' \frac{n(\mathbf{r})n(\mathbf{r}')}{|\mathbf{r} - \mathbf{r}'|}. \quad (3.108)$$

Thus,  $E_{XC}$  is obtained by subtracting from the functional  $F$  the kinetic energy functional  $T$  and the direct Coulomb energy functional (the last term in the above equation).  $E_{XC}$  carries only the effects of exchange and electronic correlations. Hohenberg and Kohn proved [60] that if the densities  $n_{\sigma}(\mathbf{r})$  are slowly varying functions, the exchange-correlation energy can be written as

$$E_{XC}[n] = \int d\mathbf{r} n(\mathbf{r}) \epsilon_{XC}[n(\mathbf{r})], \quad (3.109)$$

where  $\epsilon_{XC}$  in a uniform electron gas is the exchange-correlation energy per electron.

Now the total energy functional can be minimised with respect to the density. To this end, the energy functional (3.103) is functionally differentiated with respect to the density and this derivative is equated to zero. One obtains [67]

$$\int d\mathbf{r} \delta n(\mathbf{r}) \left\{ \frac{\delta T[n]}{\delta n(\mathbf{r})} + V(\mathbf{r}) + \frac{e^2}{\epsilon} \int d\mathbf{r}' \frac{n(\mathbf{r}')}{|\mathbf{r} - \mathbf{r}'|} + \mu_{XC}[n(\mathbf{r})] \right\} = 0, \quad (3.110)$$

with the constraint

$$\int d\mathbf{r} \delta n(\mathbf{r}) = 0. \quad (3.111)$$

In the above equations,  $\mu_{XC}[n(\mathbf{r})] = d(n\epsilon_{XC}[n(\mathbf{r})])/dn(\mathbf{r})$  is the exchange-correlation contribution to the chemical potential for the electron gas.

Solving the above equation for the density  $n(\mathbf{r})$  is equivalent to solving the single-particle Schrödinger equation

$$\left\{ -\frac{\hbar^2}{2m^*} \Delta + V(\mathbf{r}) + \frac{e^2}{\epsilon} \int d\mathbf{r}' \frac{n(\mathbf{r}')}{|\mathbf{r} - \mathbf{r}'|} + \mu_{XC}[n(\mathbf{r})] \right\} \phi_i(\mathbf{r}) = E_i \phi_i(\mathbf{r}) \quad (3.112)$$

for each electron. Thus, each electron moves in the mean field created by the external potential  $V(\mathbf{r})$ , the direct Coulomb repulsion with all other electrons, and the potential  $\mu_{XC}$  taking into account the exchange and correlation effects of the electronic system. The wave function  $\phi_i(\mathbf{r})$  is the ground state of the electron in this effective potential (the Kohn-Sham orbital).

Since the effective potential experienced by each electron depends on the behaviour of all other electrons, the equation (3.112) must be solved self-consistently. The process starts by assuming some initial density  $n(\mathbf{r})$  (e.g., constant), and calculating the wave functions  $\phi_i(\mathbf{r})$  for each electron. Next, the electronic density is recalculated as follows:

$$n(\mathbf{r}) = \sum_{i=1}^N |\phi_i(\mathbf{r})|^2, \quad (3.113)$$

and the new density is used to solve for the ground state wave functions of each electron. The procedure is repeated until the density profile  $n(\mathbf{r})$  converges, i.e., subsequent steps

do not change the density any more. The final density can be further used to calculate the total energy of the system via the energy functional  $E[n]$ .

As I mentioned before, extension of the Kohn-Sham equations to include spin is straightforward. The only modification is due to the fact that now the exchange-correlation potential  $\mu_{XC}$  depends on the spin  $\sigma$ , and one formulates separate set of Kohn-Sham equations for electrons spin up and for electrons spin down. As a result, one obtains Kohn-Sham orbitals with additional spin quantum number, and by summing their squared moduli as presented above one arrives at the densities of electrons spin up and spin down.

The Kohn-Sham equations (3.112) have been derived without any approximations, and so they describe the electronic properties of the system in the *exact* manner. However, I cannot solve them yet, since the exact form of the exchange-correlation functional  $\mu_{XC}[n(\mathbf{r})]$  is not known. Unfortunately, this functional cannot be obtained from first principles. The forms most commonly used in this context are postulated on the basis of extrapolations from the few exact results available. Frequently one assumes that the exchange-correlation potential  $\mu_{XC}$  can be locally approximated by the potential for an infinite system at constant density [104]. This is the “local spin density approximation”. The parametrisation of choice, commonly used in the context of parabolic two-dimensional quantum dots, is that of Tanatar and Ceperley [120]. These authors obtained the exchange-correlation functional of the two-dimensional gas as a Padé approximant. This approximant is constructed by fitting to the available quantum Monte Carlo results obtained for selected values of electronic density.

This necessity of postulating the exchange-correlation functional unfortunately makes the SDFT only an approximate theory. Nevertheless, it is widely used to examine the properties of many-electron quantum dots with electron numbers far exceeding the capabilities of the exact diagonalisation method. In Section 1.5 I have discussed some of the applications of the SDFT method to electronic QDs. For references and reviews of this field, I refer the reader to Refs. [11, 59, 75, 102, 104, 111, 128]. The density-functional

approach with the Thomas-Fermi-Dirac-von Weizsäcker energy functional can also be applied to arrays of quantum dots; for instance, the magnetoplasmon excitations in such arrays were analysed in Ref. [132]. In the context of comparing the SDFT method with the exact diagonalisation approach the work by Wensauer [127] is particularly interesting: the author attempts to extract the *exact* form of the exchange-correlation potential from the results of the exact diagonalisation for systems with few electrons, in which both methods can be applied with the same accuracy.

### 3.4.2 Monte Carlo methods

Let us now describe a different approach to the many-body problem, involving random sampling of the parameter space of the system and analysing the results obtained this way by statistical methods. Due to this random sampling process, this approach is widely known as the quantum Monte Carlo method (QMC). In reality one can name several quantum Monte Carlo methods, differing in the definition of the parameter space being sampled. A review of these methods can be found in several papers by D. Ceperley [29], in which the author presents the main principles of the variational QMC, path integral QMC, Green's function QMC and the diffusion QMC. Each of these techniques is usually used in a slightly different context. For instance, in the variational QMC one defines a trial variational wave function of the system, and, using the variational principle, one tries to find the minimum of the expectation value of the Hamiltonian in this state. The wave function usually depends on several parameters, whose optimal values must be found, and the calculation of the expectation value of the energy usually involves calculating a multi-dimensional integral. Both tasks can be accomplished using Monte Carlo sampling. In path-integral QMC all the possible paths the system can take in its evolution are explored, usually using the rejection algorithm of Metropolis *et al.* [84]. Here, however, I shall focus only on the quantum diffusion Monte Carlo technique (QDMC), because it is frequently used to study the properties of systems of many interacting electrons confined

in quantum dots.

Perhaps the best introduction to the subject can be found in Ref. [3], where Anderson describes the application of QDMC to study the properties of the  $H_3^+$  molecule, composed of three protons localised in the corners of an equilateral triangle, and two interacting electrons with antiparallel spins moving in their potential. The description starts with the simple one-dimensional time-dependent Schrödinger equation, written for a single particle moving in a potential  $V(x)$ :

$$-i\hbar \frac{\partial \psi(x, t)}{\partial t} = \frac{\hbar^2}{2m^*} \frac{\partial^2 \psi(x, t)}{\partial x^2} - V(x)\psi(x, t). \quad (3.114)$$

The key point of the method consists in introducing the imaginary time  $\tau$ , defined as

$$\tau = i \frac{t}{\hbar}. \quad (3.115)$$

The Schrödinger equation written in terms of this parameter takes the form

$$\frac{\partial \psi(x, \tau)}{\partial \tau} = \frac{\hbar^2}{2m^*} \frac{\partial^2 \psi(x, \tau)}{\partial x^2} - V(x)\psi(x, \tau). \quad (3.116)$$

Clearly, the above differential equation can be easily integrated over the imaginary time, and its solution will have the form

$$\psi(x, \tau) = \psi(x)e^{-E\tau}, \quad (3.117)$$

where the orbital part  $\psi(x)$  of the wave function and the energy  $E$  must be obtained by solving the stationary Schrödinger equation, defined by the right-hand side of Eq. (3.116).

Note that the form of Equation (3.116) is similar to that of the diffusion equation in real time:

$$\frac{\partial C}{\partial t} = \mathcal{D} \frac{\partial^2 C}{\partial x^2} - kC, \quad (3.118)$$

where  $\mathcal{D}$  is the diffusion constant,  $C$  is the distribution of diffusing particles, and  $k$  is a rate term, describing the decay of the population of diffusing particles. The idea of the QDMC technique is to use this analogy, and model the imaginary-time evolution of the system as the game of chance, using “ $\psi$  particles” as random walkers.

By mapping the equation (3.116) onto the equation (3.118) one sees immediately that for each random walker  $\psi$  situated at the position  $x$  the “diffusion constant”  $\mathcal{D} = \frac{\hbar^2}{2m^*}$ , and the “rate term”  $k = V(x)$ , i.e., it is equal to the value of the potential  $V$  at the point where the random walker is. The simulation is organised in such a way that the imaginary time  $\tau$  is advanced in steps  $\Delta\tau$ , and during this time interval the random walker changes its position by  $\Delta x$ . These quantities are, of course, not independent; according to the Einstein relation [94]

$$\frac{1}{2} \frac{(\Delta x)^2}{\Delta\tau} = \mathcal{D}. \quad (3.119)$$

In the absence of the rate term  $k$  the diffusion equation can be solved analytically, and the probability that the random walker takes the step of length  $\Delta x$  in time interval  $\Delta\tau$  exhibits a Gaussian distribution:

$$W(\Delta x) = \frac{1}{\sqrt{2\pi}\sigma} \exp\left(-\frac{(\Delta x)^2}{2\sigma^2}\right), \quad (3.120)$$

where the parameter  $\sigma = \sqrt{2\mathcal{D}\Delta\tau}$ . This is why in this game of chance after each time step  $\Delta\tau$  one moves the random walkers by distances  $\Delta x$  selected at random according to the Gaussian distribution, and accounts for the rate term (i.e., the existence of the external potential) by conditional *deaths* or *births* of random walkers.

I can now formulate the general QDMC algorithm for my problem, posed by defining the Schrödinger equation for a  $M$ -particle system

$$\frac{\partial\psi}{\partial\tau} = \left[ \sum_{i=1}^M \frac{\hbar^2}{2m_i} \Delta_i - (V - V_{ref}) \right] \psi = -(E - V_{ref})\psi. \quad (3.121)$$

1. In the first, preparatory step, one creates  $N$  random walkers distributed randomly in real space. If the problem has a single-particle nature in three dimensions, each random walker will be remembered as a triplet of numbers, defining its coordinates. If the problem involves more particles, say  $M$ , each random walker will have  $3M$  coordinates, defining the position of each particle in space.
2. Now the simulation time is advanced by  $\Delta\tau$  (this time interval is chosen by the user). All coordinates of each random walker are changed by the step  $\Delta x$  selected



at random with the Gaussian distribution as described above. Of course, steps for each coordinate of each random walker are chosen independently, so that in each case we deal with the real random walk in  $3M$ -dimensional space.

3. Next one accounts for the rate term  $k$ . In this simulation, as already mentioned, the value of this rate term equals to the value of the potential at coordinates of each random walker, and is clearly different for each walker. In general, it is not just the confinement potential, but it also contains all relevant particle-particle interactions. For instance, for my interacting electrons the rate term will comprise both the value of the parabolic potential corresponding to a given distribution of electrons in space, but also all Coulomb interactions between each pair of electrons.

The probability of birth or death is calculated by comparing the full potential  $V$  of a given walker to a certain reference potential  $V_{ref}$ , used to control the population of walkers; I shall define this potential later. Here let us only state that the probability of birth for each walker is

$$P_B = -(V - V_{ref})\Delta\tau \quad \text{if } V < V_{ref},$$

$$P_B = 0 \quad \text{if } V \geq V_{ref},$$

and the probability of death is

$$P_D = (V - V_{ref})\Delta\tau \quad \text{if } V > V_{ref},$$

$$P_D = 0 \quad \text{if } V \leq V_{ref}.$$

For each walker one select at random a number from the region  $(0, 1)$  (with uniform distribution) and compares it to the above probabilities. If this number is smaller than  $P_B$ , another, new walker is introduced at the position of the current one (birth), and if it is smaller than  $P_D$ , the current walker is removed from the population. Note that by doing so I, in general, change the number  $N$  of random walkers.

4. The procedure outlined in points 2 and 3 is repeated until the population of random walkers reaches the steady state distribution.

I must now develop tools allowing me to derive meaningful physical information from the random walk procedure. First of all, let us define the reference potential  $V_{ref}$  as

$$V_{ref} = V_{avg} - \frac{N - N_P}{N_P \Delta\tau}. \quad (3.122)$$

The number  $N_P$  is the target number of random walkers. If the current population  $N$  is smaller than  $N_P$ , the reference potential will favour births of walkers; if  $N > N_P$ , the reference potential will favour their deaths. In the above formula,  $V_{avg}$  is the average potential of random walkers, calculated by adding the potential of each walker and dividing by the current number of walkers  $N$ . Second, it can be proved [3] that upon reaching the steady-state distribution, the total energy of the system is simply  $E = V_{avg}$ .

The procedure I have just described contains no approximations, and therefore should give *exact* results within the numerical accuracy of the algorithm. In practice, in order to be able to perform a meaningful statistical study, it is advisable to take large population of walkers and small time steps  $\Delta\tau$ . Another improvement in the efficiency of this algorithm can be introduced by the so-called *importance sampling* [3]. In real systems the random walkers are usually distributed nonuniformly, reflecting the fact that usually the probability of finding the particles is larger in some areas, and smaller in others. Therefore, it is not efficient to sample all these regions in the same way: regions, where the wave function is expected to assume the largest values, should be sampled preferentially. To introduce this importance sampling, one usually prepares a trial function, reflecting the expected steady-state distribution of walkers, and one modifies the QDMC algorithm so that only the *difference* between the actual and the trial distributions is calculated.

The quantum diffusion Monte Carlo algorithm can be applied directly to single particle problems, and problems of many interacting bosons. However, in the case of many interacting fermions it is necessary to modify the approach in order to account for the antisymmetry of the wave function of the system. From the above description it is clear that the distribution of the random walkers is a measure of the wave function distribution in the system, but the method cannot yield negative distributions. But for many-fermion

systems there must be regions, where the total wave function of the system assumes positive values, and other regions, where it is negative. The QDMC algorithm in such cases is constructed in such a way that the motion of random walkers is constrained to areas, where the function is positive, and, at the same time, only those areas that are not connected via the permutation operator. This is an important difficulty, since in order to be able to execute the algorithm, one must know in advance where the nodes of the total wave function are so that the motion of walkers can be restricted only to the appropriate regions between nodal surfaces. To achieve this goal, several techniques were developed, usually involving some kind of trial wave function  $\psi_T$  as an input [3, 23]. The trial function can be prepared, e.g., by performing the SDFT calculation first, arranging the Kohn-Sham orbitals in a single Slater determinant, and determining the nodal surfaces of such many-particle function [22, 49].

Another difficulty appears in treatments of interacting fermions in the presence of an external magnetic field. Since in such cases the real-space Hamiltonian exhibits a broken time-reversal symmetry, the wave functions are usually complex, and the magnetic field usually couples to their phase [93]. In this case it is possible to write the complex Schrödinger equation as a set of two coupled real equations: one for the modulus, and one for the phase of the wave function, and the equation for the modulus is already of the bosonic nature, i.e., does not suffer from the sign problem. The procedure here is to make a choice for the phase, and solve for the modulus exactly (that is, exactly within this particular choice of the phase) using the diffusion algorithm.

The QDMC and other Monte Carlo techniques are extensively used in the context of many-electron quantum-dot systems [22, 40]. In the paper discussing the exact diagonalisation method optimised for the harmonic-oscillator basis set (Section 3.3.2), we have briefly presented a comparison of energies obtained with this method and with QDMC, and shown an excellent agreement of the results of these two techniques. However, it is clear that the QDMC method is capable of handling much larger systems than the

exact diagonalisation. The only real difficulty arises in constructing the fixed-node or fixed-phase schemes, whose level of complexity increases with the increase of the number of electrons.